High-order parameterization of stable/unstable manifolds for long periodic orbits of maps

J.L. Gonzalez * [1] and J.D. Mireles James †[2]

[1,2]Florida Atlantic University, Department of Mathematical Sciences

August 16, 2016

Abstract

We consider the problem of computing stable/unstable manifolds attached to periodic orbits of maps, and develop quasi-numerical methods for polynomial approximation of the manifolds to any desired order. The methods avoid function compositions by exploiting an idea inspired by multiple shooting schemes for periodic orbits. We consider a system of conjugacy equations which characterize chart maps for the local stable/unstable manifold segments attached to the points of the periodic orbit. We develop a formal series solution for the system of conjugacy equations, and show that the coefficients of the series are determined by recursively solving certain linear systems of equations. We derive the recursive equations for some example problems in dimension two and three, and for examples with both polynomial and transcendental nonlinearities. Finally we present some numerical results which illustrate the utility of the method and highlight some technical numerical issues such as controlling the decay rate of the coefficients and managing truncation errors via a-posteriori indicators.

1 Introduction

In this work we develop a general semi-numerical method for computing high order polynomial parameterizations of local stable/unstable manifolds attached to periodic orbits of maps. Our approach is based on the Parameterization Method of [1, 2, 3], a general functional analytic framework for studying invariant manifolds. The main idea of the Parameterization Method is to study a certain invariance equation which conjugates the linearized dynamics at the fixed point to the nonlinear dynamics on the invariant manifold (see Equation (4)). The method gives the dynamics on the invariant manifold in addition to the embedding. Moreover, the parameterization is not required to be the graph of a function, and it is possible to follow folds in the embedding. The invariance equation also provides a convenient notion of defect, which is exploited in the a-posteriori error analysis.

A period-N orbit for a map $f\colon \mathbb{R}^M \to \mathbb{R}^M$ is a fixed point of the map f^N (f composed with itself N times), and in principle one could compute invariant manifolds for period-N points by applying the Parameterization Method to the map f^N. In practice however, the nonlinearity of the composition f^N is exponentially more complicated than the nonlinearity of f. The novelty of the present work is a *composition free* Parameterization Method for manifolds attached to periodic points which exploits a simple multiple shooting scheme.

*J.L.G. partially supported by NSF grant DMS - 1318172 Email: jorgegonzale2013@fau.edu

†J.M.J partially supported by NSF grant DMS - 1318172 Email: jmirelesjames@fau.edu

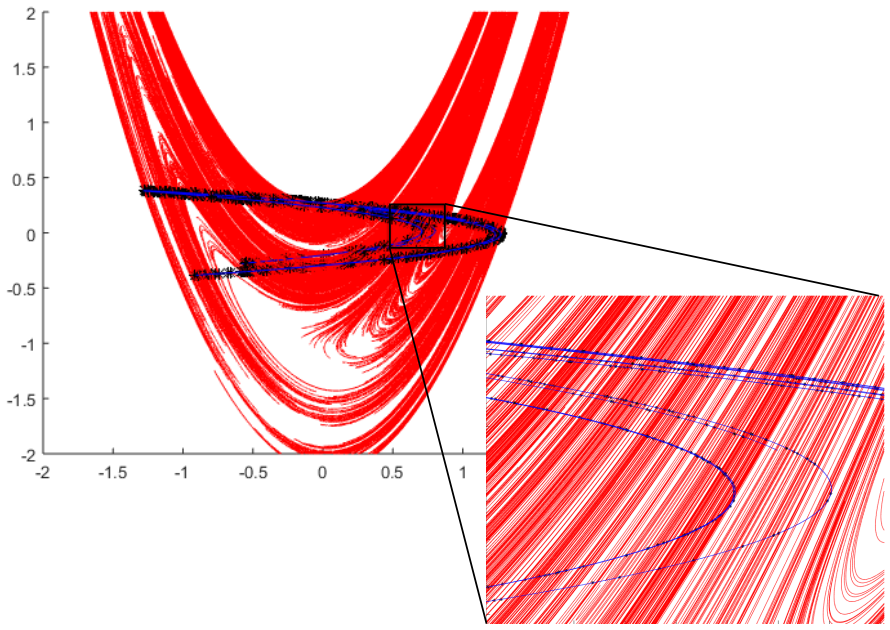

Figure 1: Periodic orbits and their attached invariant manifolds for the Hénon map: the figure illustrates the parameterized local unstable/stable manifolds attached to a collection of periodic orbits. The collection contains orbits whose periods range from 2-16. The periodic orbits are black, unstable manifolds are blue, and stable manifolds are red. It is clear from the picture that the stable/unstable manifolds intersect many times. The picture is generated by evaluating a collection of polynomial parameterizations for the local stable/unstable manifolds of the periodic orbits, and does not involve any iteration of the map itself.

More precisely if $p_1, \ldots, p_N \in \mathbb{R}^M$ is a periodic orbit with $m \leq M$ stable (or unstable) eigenvalues, then our method simultaneously finds the Taylor approximations of some functions $P_1, \ldots, P_N \colon \mathbb{R}^m \to \mathbb{R}^M$ having that P_j parameterizes a local stable (or unstable) manifold attached to p_j for each $1 \leq j \leq N$. The Taylor approximation is computed numerically to any desired order. Just as in a multiple shooting scheme for the periodic orbit itself, our system of invariance equations involves no compositions, hence the nonlinearity determining the stable/unstable manifold for the periodic orbit is only as complicated as the original nonlinearity of the model (see Equation (8)).

In order to illustrate the utility of the method implement it for several application problems in dimensions two and three. We discuss a number of computations for one and two dimensional manifolds associated with periodic orbits of period up to 100 for a planar and spatial Hénon type map. We also show that application of the method is not limited to polynomial maps by computing stable/unstable manifolds for some periodic orbits of the "the standard map", a system having a trigonometric nonlinearity.

Remark 1.1 (Illustration of results)**.** Figures 1 and 2 illustrate some results obtained using the methods of the present work. The first figure shows parameterized local stable/unstable

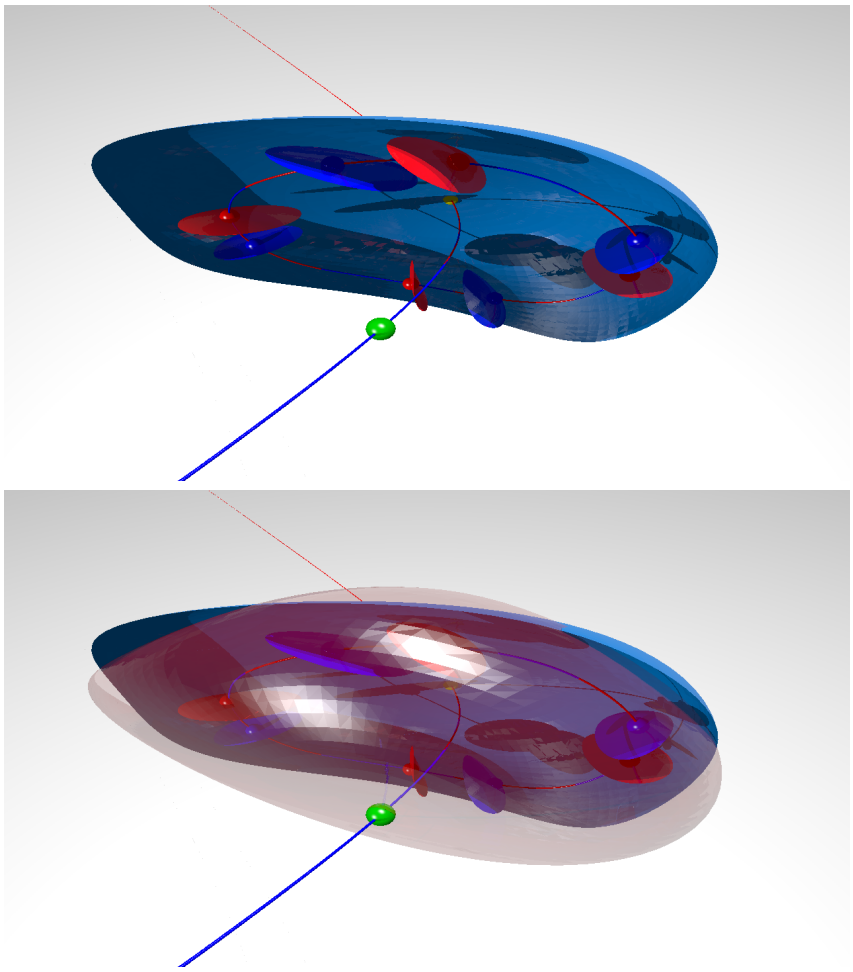

Figure 2: Period four vortex bubble in the Lomelí map: Top - the image illustrates the parameterizations of several one and two dimensional stable (red) and unstable (blue) manifolds. The largest surface is the unstable manifold of a fixed point. There are also two hyperbolic period four orbits: one with two dimensional unstable/one dimensional stable manifolds, and the other vice verse. Bottom - same picture but with the stable manifold of the second fixed point included. The stable and unstable manifolds of the two fixed points form a "bubble" enclosing the period four points and their invariant manifolds.

manifolds attached to a collection of periodic orbits for the Hénon map at the classical parameter values. More precisely, the collection of contains 1 period two, 1 period four, 2 period six, 4 period seven, 7 period eight, 6 period nine, 10 period ten, 14 period eleven, 13 period twelve, 23 period thirteen, 9 period fourteen, 21 period fifteen, and 14 period sixteen orbits. Each manifold is approximated to Taylor order 25, and the decay rate of the Taylor coefficients is controlled adaptively in order to insure that the last coefficients in this expansion are small. The a-posteriori error for each manifold is below 10^{-14}.

The second figure shows results from a similar computation involving two fixed points and two period four orbits of the three dimensional Lomelí map. Again the manifolds are approximated to Taylor order 25 and the a-posteriori error is small. More details for these

and other computations are found in Section 4.

The curves and surfaces shown in the figures are obtained by evaluating the Taylor polynomials. The polynomials are computed using the methods developed in Section 3 and implemented as discussed in Section 4. No iteration of the maps is used in the generation these images.

Remark 1.2 (A-posteriori analysis versus validated numerics)**.** As mentioned above, one of the strengths of the Parameterization Method leads is that it provides a notion of a-posteriori analysis (or defect), i.e. since the desired parameterizations solve an operator equation we can always "plug" our approximation back into the operator equation and asses (via some convenient choice of norm) how well we have done in solving the equation. In the present work we use the a-posteriori error as an indicator of the quality of our computations.

Of course small defects do not imply small truncation errors, and is desirable to have a more refined a-posteriori analysis. Indeed, via a blend of pen and paper analysis with deliberate control of round-off errors, it is possible to obtain mathematically rigorous computer assisted error bounds associated with the polynomial approximations. Several woks in this vein, for both finite and infinite dimensional dynamical systems, are [4, 5, 6, 7, 8, 9]. Developing validated numerics for the techniques of the present work is the topic of an upcoming study by the authors.

2 Background

Let $x = (x_1, \ldots, x_M) \in \mathbb{R}^M$ denote a point in Euclidean M-space, and endow $\mathbb{R}^M$ with the norm

$$\|x\| := \max_{1 \le j \le M} |x_j|,$$

where $|\cdot|$ denotes the usual absolute value. Let

$$B_r^M(x) := \left\{ y \in \mathbb{R}^M : \|x - y\| < r \right\},$$

denote the ball (actually cube) of radius r about x in this norm. If $E \subset \mathbb{R}^M$ is compact and $x \in \mathbb{R}^M$, define

$$d(x, E) := \inf_{y \in E} \|x - y\|,$$

the distance from x to E.

When discussing power series we employ the following notation. If $P \colon \mathbb{R}^m \to \mathbb{R}^M$ is analytic at $p_0 \in \mathbb{R}^M$ then P has a power series representation

$$P(\theta) = \sum_{|\alpha|=0}^{\infty} p_\alpha \theta^\alpha = \sum_{\alpha_1=0}^{\infty} \cdots \sum_{\alpha_m=0}^{\infty} p_{\alpha_1,\ldots,\alpha_m} \theta_1^{\alpha_1} \ldots \theta_m^{\alpha_m},$$

where $\alpha = (\alpha_1, \ldots, \alpha_m) \in \mathbb{N}^m$ is an m dimensional multi-index,

$$|\alpha| := \alpha_1 + \ldots + \alpha_m,$$

$p_\alpha \in \mathbb{R}^M$ for each α, and

$$\theta^\alpha := \theta_1^{\alpha_1} \ldots \theta_m^{\alpha_m}.$$

2.1 Stable/unstable manifold for discrete time dynamical systems

Consider a diffeomorphism $f : \mathbb{R}^M \to \mathbb{R}^M$ with fixed point p. (All of the examples considered in the present work are analytic maps with analytic inverse, i.e. analyticmorphism). Suppose that p is a hyperbolic fixed point of f, i.e. that no eigenvalues of $Df(p)$ lie on the unit circle. Then there are $m_s, m_u \in \mathbb{N}$ with $m_s + m_u = M$ so that $Df(p)$ has m_s stable eigenvalues and m_u unstable eigenvalues (counted with multiplicity). We then label the eigenvalues as $\lambda^s_1, \ldots, \lambda^s_{m_s}, \lambda^u_1, \ldots, \lambda^u_{m_u}$ with

$$0 < |\lambda^s_{m_s}| \leq \ldots |\lambda^s_1| < 1 < |\lambda^u_1| \leq \ldots |\lambda^u_{m_u}|.$$

Let $\xi^u_1, \ldots, \xi^u_{m_u}, \xi^s_1, \ldots, \xi^s_{m_s} \in \mathbb{R}^M$ denote a choice of linearly independent (possibly generalized) eigenvectors.

Let $U \subset \mathbb{R}^M$ be an open neighborhood of p. The local stable set of p relative to U is

$$W^s_{\text{loc}}(p, U) := \left\{ x \in \mathbb{R}^M : f^n(x) \in U \text{ for all } n \geq 0 \right\}.$$

By the Stable Manifold Theorem (see for example [10] for discussion and proof) there exists an open neighborhood $V \subset \mathbb{R}^M$ of p so that

(i) The local stable set $W^s_{\text{loc}}(p, V)$ is a smooth, embedded, m_s-dimensional disk. If f is analytic then the embedding is analytic.

(ii) $W^s_{\text{loc}}(p, V)$ is tangent to the stable eigenspace of $Df(p)$ at p, i.e. the vectors $\xi^s_1, \ldots, \xi^s_{m_s}$ span the tangent space of $W^s_{\text{loc}}(p, V)$ at p.

(iii) If $x \in W^s_{\text{loc}}(p, V)$ then

$$\lim_{n\to\infty} f^n(x) = p.$$

We refer to any local stable set $W^s_{\text{loc}}(p, V)$ satisfying $(i) - (iii)$ above as a local stable manifold for p. We say that $W^s_{\text{loc}}(p)$ is a local stable manifold at p if $W^s_{\text{loc}}(p) = W^s_{\text{loc}}(p, V)$ satisfies $(i) - (iii)$ above with V some open neighborhood of p. Note that if $W^s_{\text{loc}}(p, V)$ has $(i) - (iii)$ above and $B^M_r(p) \subset V$, then $W^s_{\text{loc}}(p, B^M_r(p))$ has $(i) - (iii)$ as well, i.e. local stable manifolds are not unique.

Since f is invertible we can, given any local stable manifold $W^s_{\text{loc}}(p, V)$, define the set

$$W^s(p) = \bigcup_{n=0}^{\infty} f^{-n}\left[W^s_{\text{loc}}(p)\right] = \left\{ x \in \mathbb{R}^M \mid f^n(x) \to p \text{ as } n \to \infty \right\}. \tag{1}$$

The resulting set $W^s(p)$ is a globally invariant manifold (which may not be an imbedded disk). We refer to $W^s(p)$ as *the* stable manifold of p, as $W^s(p)$ does not depend on the choice of local stable manifold.

These considerations applied to f^{-1} at p let us define local unstable manifolds, which we denote by $W^u_{\text{loc}}(p)$ with analogous definition. (We remark that if p is a hyperbolic fixed point of a smooth map f then f^{-1} exists at least locally, and the assumption above that f is a diffeomorphism on $\mathbb{R}^M$ is not actually needed to define the local unstable manifold. However this fact is not used in the present work). The set

$$W^u(p) = \bigcup_{n=0}^{\infty} f^{n}\left[W^u_{\text{loc}}(p)\right] = \left\{ x \in \mathbb{R}^M \mid f^{-n}(x) \to p \text{ as } n \to \infty \right\},$$

is a unique globally defined invariant manifold which we refer to as *the* unstable manifold of p.

Remark 2.1 (Linear approximation of the local stable/unstable manifolds)**.** Even when the map $f\colon \mathbb{R}^M \to \mathbb{R}^M$ is explicitly known, closed form expressions for the local stable/unstable manifolds $W^{s,u}_{\rm loc}(p)$ are rarely available. In applications we are interested in approximating these manifolds, and part (ii) of the Stable Manifold Theorem provides a first order approximation. More precisely, suppose that the vectors $\xi^s_1, \ldots, \xi^s_{m_s}$ are all scaled to have length one and define the $M \times m_s$ matrix

$$[\xi^s_1 | \ldots | \xi^s_{m_s}] = A_s,$$

i.e. A_s is the matrix with columns given by the (generalized) eigenvectors. Then the parameterization $P^1\colon \mathbb{R}^{m_s} \to \mathbb{R}^M$ given by

$$P^1(\theta) := p + A_s\theta, \qquad\qquad \theta := (\theta_1, \ldots, \theta_{m_s}),$$

approximates $W^s_{\rm loc}(p)$ to first order. More precisely, let

$$B^{m_s}_\delta(0) := \{\theta \in \mathbb{R}^{m_s} : \|\theta\| < \delta\}.$$

The restriction of P^1 to $B^{m_s}_\delta(0)$ is a quadratically good approximation of the stable manifold, in the sense that

$$\sup_{\theta \in B^{m_s}_\delta(0)} \operatorname{dist}\left(P^1(\theta), W^s_{\rm loc}(p)\right) \le C\|\theta\|^2,$$

though in practice more work is required in order to obtain estimates on the magnitude of C. Nevertheless, combining the observation above with Equation (1) leads to various algorithms for approximating $W^s(p)$. This point is discussed in more detail in Section 2.3. Similar considerations lead to a linear approximation of the local unstable manifold by the unstable (generalized) eigenvectors.

Remark 2.2. To define the linear approximation P^1 in Remark 2.1 it is necessary to fix a choice of scalings for the (generalized) eigenvectors, and of course this choice is not unique. In general the size of the neighborhood on which the linear approximation gives quadratically good approximation depends on the choice of scalings. For example, in Remark 2.1 we would have obtained exactly the same results by taking the (generalized) eigenvectors to have scalings

$$\|\xi^s_j\| = \delta, \qquad\qquad 1 \le j \le m_s,$$

and restricting the domain of P^1 to the unit ball $B^{m_s}_1(0)$.

This non-uniqueness is inherent in all schemes for approximating the stable manifold, and actually plays an important role in the sequel. The issue is not surprising as the non-uniqueness appears already in the definition of the local stable manifold (i.e. there is one local stable manifold for every appropriate choice of neighborhood of the fixed point). In the case of the linear approximation the choice of scalings is more or less arbitrary and we might as well take unit vectors as in Remark 2.1. However, when we study high order approximations we will see that that the freedom of choice in scaling the (generalized) eigenvector allows us to control the decay of the Taylor coefficients of the high order approximation. Manipulating the decay rates is in turn useful for stabilizing numerical computations.

2.2 Series expansion of a conjugating chart map: the Parameterization Method

Suppose that f, p, and m_s are as in Section 2.1. Throughout the remainder of the section we assume that $m = m_s > 0$ and let $\lambda_1, \ldots, \lambda_m$, and $\xi_1, \ldots, \xi_m$ denote respectively the

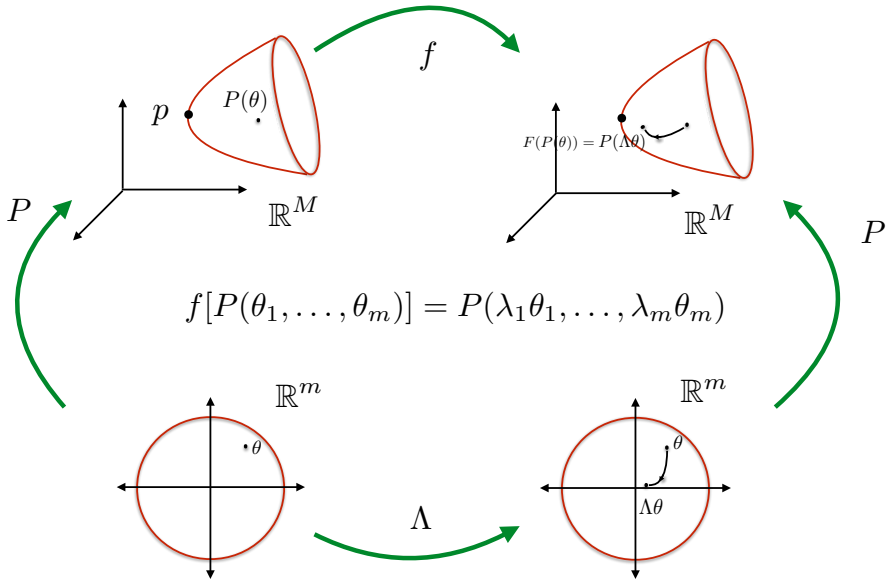

Figure 3: Cartoon illustrating the conjugacy relation codified by Equation (4).

stable eigenvalues and an associated choice of linearly independent (generalized) eigenvectors. Again: by the stable manifold theorem there is a local stable manifold $W^s_{\text{loc}}(p)$, which is geometrically a smooth embedded disk tangent to the stable (generalized) eigenspace at $p \in \mathbb{R}^M$. We are interested in smooth injective maps $P\colon B_1^m(0) \to \mathbb{R}^M$ having that

$$P(0) = p, \qquad \text{and} \qquad \frac{\partial}{\partial \theta_j} P(\theta) = \xi_j, \qquad \text{for each } 1 \leq j \leq m, \tag{2}$$

and

$$P\left[B_1(0)^m\right] \subset W^s(p), \tag{3}$$

i.e. charts for the local stable manifold. Clearly if P is one such chart, then any reparameterization of P is again a chart. So, the parameterization P just discussed cannot be unique, and we are free to impose additional constraints.

The idea of *the Parameterization Method* [1, 2, 3] is to look for a smooth function $P\colon B_1^m(0) \to \mathbb{R}^M$ satisfying the first order constraints of Equation (2), and solving the conjugacy equation

$$f[P(\theta_1, \ldots, \theta_m)] = P(\lambda_1\theta_1, \ldots, \lambda_m\theta_m), \tag{4}$$

for all $\theta \in B_1^m(0)$. Several useful results for the Parameterization Method are summarized below. First we need the following definition.

Definition 2.3 (Non-resonant eigenvalues)**.** We say that the stable eigenvalues $\lambda_1, \ldots, \lambda_m$ are *non-resonant* if

$$\lambda_1^{\alpha_1} \cdot \ldots \cdot \lambda_m^{\alpha_m} \neq \lambda_j, \qquad \text{with } 1 \leq j \leq m,$$

for all $\alpha = (\alpha_1, \ldots, \alpha_m) \in \mathbb{N}^m$, i.e. if no product of positive powers of the stable eigenvalues is again a stable eigenvalue.

First we note that, despite first appearances, Definition 2.3 imposes only a finite number of constraints on the eigenvalues. To see this let

$$\mu_* = \min_{1\leq j\leq m} |\lambda_j|, \qquad \text{and} \qquad \mu^* = \max_{1\leq j\leq m} |\lambda_j|,$$

denote respectively the smallest and largest moduli of the stable eigenvalues, and note that for any multi-index $\alpha \in \mathbb{N}^m$ we have the bound

$$\begin{aligned} |\lambda_1^{\alpha_1} \cdot \ldots \cdot \lambda_m^{\alpha_m}| &\leq (\mu^*)^{\alpha_1} \cdot \ldots \cdot (\mu^*)^{\alpha_m} \\ &= (\mu^*)^{|\alpha|}. \end{aligned}$$

Then a resonance is impossible for all $\alpha \in \mathbb{N}^m$ with

$$(\mu^*)^{|\alpha|} < \mu_*,$$

and we conclude that a necessary condition for a resonance is

$$2 \leq |\alpha| \leq \frac{\ln(\mu_*)}{\ln(\mu^*)}.$$

Then checking that a collection of stable (or unstable) eigenvalues is non-resonant is a finite check.

Definition 2.4 (Eigenvector scalings)**.** Suppose that

$$\|\xi_1\| = s_1, \ldots, \|\xi_m\| = s_m.$$

We refer to the collection of numbers $s_1, \ldots, s_m > 0$ as the scalings of the (generalized) eigenvectors, and write

$$s = \max_{1\leq j\leq m} (s_j).$$

The following theorem summarizes a number of basic results. **Note: from this point forward we impose the additional assumption that the differential is diagonalizable** (see however Remark 2.6 below). Proofs of these results can be extracted from the much more general discussion in [1].

Lemma 2.5. *Let $f\colon \mathbb{R}^M \to \mathbb{R}^M$ be an invertible map and $p \in \mathbb{R}^M$ be a fixed point of f. Suppose that f is differentiable in a neighborhood of p, and assume that the differential $Df(p)$ is a diagonalizable matrix. Let $\lambda_1, \ldots, \lambda_m \in \mathbb{C}$ denote the stable eigenvalues of $Df(p)$, and $\xi_1, \ldots, \xi_m \in \mathbb{R}^M$ denote an associated choice of linearly independent eigenvectors.*

- *If $P\colon B_1^m(0) \to \mathbb{R}^M$ is a smooth solution of Equation (4) satisfying the first order constraints given by Equation (2), then P is a chart map for a local stable manifold of p.*
- *If $\lambda_1, \ldots, \lambda_m$ are non-resonant, in the sense of Definition 2.3, then there exists an $\epsilon > 0$ so that for every choice of eigenvectors with scalings $s_1, \ldots, s_m$ as in Definition 2.4 having $s_1, \ldots, s_m \leq \epsilon$, Equation (4) has a solution $P\colon B_1^m(0) \to \mathbb{R}^M$ subject to the constraints of Equation (2). The solution P is unique up to the choice of the eigenvectors.*
- *If $f \in C^k(\mathbb{R}^M)$ then $P \in C^k(B_1^m(0), \mathbb{R}^M)$ as well. $k \in \{\infty, \omega\}$ are included in this claim.*

Now assume that f is analytic near p. Then Lemma 2.5 says that for some choice of eigenvector scalings a parameterization P solving Equation (4) exists, and that the function P is analytic. Then it is natural to look for a power series solution

$$P(\theta) = \sum_{|\alpha|=0}^{\infty} p_\alpha \theta^\alpha.$$

P satisfies the first order constraints of Equation (2) if we require that

$$p_{\mathbf{0}} = p,$$

and

$$p_{e_j} = \xi_j, \qquad \text{for} \quad 1 \leq j \leq m_s,$$

where $\mathbf{0} = (0, \ldots, 0) \in \mathbb{N}^{m_s}$ is the m_s-dimensional multi-index and $e_j = (0, \ldots, 1, \ldots, 0)$ are the standard basis vectors with 1 in the j-th entry and zeros elsewhere.

In order to work out the higher order coefficients p_α with $|\alpha| \geq 2$ we expand Equation (4) in terms of this power series, and match like powers of θ. This computation results in the *homological equation*

$$\left[Df(p) - \lambda_1^{\alpha_1} \cdots \lambda_{m_s}^{\alpha_{m_s}} \mathrm{Id}\right] p_\alpha = s_\alpha, \tag{5}$$

where s_α is a function only of the coefficients p_β with $|\beta| < |\alpha|$, and the form of s_α is completely determined by the nonlinearity of f. Equation (5) says that the Taylor coefficients of the desired parameterization solve linear equations.

Note that as long as the eigenvalues are non-resonant, in the sense of Definition 2.3, then the homological equations (5) are recursively uniquely solvable to any desired order, i.e. the parameterization P is formally well defined. If s_α is known explicitly then numerical algorithms for computing the parameterization P are obtained by solving Equation (5) to the desired order. Determination of the specific form of s_α is a problem dependent issues best illustrated by examples.

Remark 2.6.

- These developments apply to the unstable manifold with only the obvious changes, i.e. one considers exactly the same conjugacy given in Equation (4) and is led to exactly the same homological equations as given by Equation (5), the only change being that stable eigenvalues/eigenvectors must be replaced by the unstable eigenvalues/eigenvectors. General treatment of the Parameterization Method is found in the work of [1, 2, 3]. Several papers which focusing on numerical aspects of the Parameterization Method for stable/unstable manifolds of fixed points for maps are [11, 12, 5, 13, 14]. Many additional extensions and applications of these techniques, as well as a thorough discussion of the literature, are found in the recent book of [15].

- In a particular problem the eigenvalues could admit a resonance (or a finite number of resonances). In this case, even if f is analytic, it is not possible to analytically conjugate to the linear dynamics. Yet this is not the end of the story, as the method can still succeed after modifying the conjugacy. In fact, one conjugates to a polynomial rather than linear map, and the polynomial is chosen in order to "kill off" the resonant terms. Similar remarks hold in the non-diagonalizable case, i.e. when we have repeated eigenvalues/generalized eigenvectors. These degenerate cases are worked out in full detail in [1]. The end result is that the Parameterization Method always applies, once resonances are accounted for. See also the work of [8] for numerical implementation, and a-posteriori analysis of the resonant cases. More general non-resonance conditions are studied in [16].

2.3 Related literature: numerical computation of local stable/unstable manifolds and growing or continuing the global manifold

There are two issues or steps which have to be considered in any discussion of the numerical computation of a stable/unstable manifold. The first issue is approximating the local stable/unstable manifold, and the second issue is choosing a strategy for growing a larger portion of the manifold (i.e. continuing or globalizing the manifold) given a local patch from the first step. These two steps have their own distinct flavors, and a growing body of literature is devoted to each.

The simplest approximation of the local stable/unstable manifold is the linear approximation by the eigenspace mentioned already in Remark 2.2. The linear approximation is widely used as it is sufficient for the needs of many applications. The idea of studying an invariance equation to obtain the jets of an invariant object appears as early as the work of Poincar'e (see for example the historical discussion in Appendix A of [3]), and numerical methods based on this idea go back to the work of [17]. See also the lecture notes of [18]. Since then many authors have expanded this line of research and a small (and incomplete) sample of works which focus on high order numerical approximation of stable/unstable manifolds attached to fixed points of maps includes [19, 12, 14, 9]. The works just mentioned discuss many additional references. The reader interested in these techniques should consult the recent book of [15] for much more complete overview of the literature, and many generalizations to quasi-periodic solutions, their invariant sets, and applications to ordinary differential equations.

Given a good local approximation of the stable/unstable manifold one uses techniques such as those developed in [20, 21] in order to increase the manifold. For the case of differential equations we also mention the method of geodesic level sets [22, 23, 24], the method of BVP continuation of trajectories [25], the method of fat trajectories [26], the PDE formulation of [24], as well as the set oriented methods of [27]. The methods of the last reference cited apply to maps as well. In many applications the continuation/globalization methods just mentioned can be "seeded" with only the linear approximation of the stable/unstable manifold by the associated stable/unstable eigenspace in order to produce the desired results, however none of these methods depend on this (i.e. they could as well be "seeded" with larger local patches of manifold given by some high order approximation).

The two studies [28, 29] explore the possibility of building adaptive continuation methods seeded with high-order parameterizations of the local stable/unstable manifolds. In these works the local manifold is computed to any desired order using the Parameterization Method (much as in the present work) and then a larger portion of the manifold is grown by adaptively iterating a mesh composed of Bézier triangle patches. These works illustrate nicely what can be achieved by combining the Parameterization method with sophisticated continuation techniques.

In applications computing stable/unstable manifolds is a first step toward understanding global dynamics of nonlinear systems. We refer for example to the numerical studies of global bifurcations and preturbulence for the Lorenz system [30, 31], global consequences of bifurcations at infinity such as α-flips [32], and global invariant manifolds near a Shilnikov bifurcation in a laser model [33]. The interactions between Julia sets and stable/unstable manifolds are studied numerically in [34]. Dynamical transport and design of low energy transport in celestial mechanics, as discussed in [35, 36, 37, 38, 39, 37], is an outstanding example of the use of stable/unstable manifolds in applications. See also the work of [40, 41, 42, 43] on weak stability boundaries and geometric instability in hamiltonian systems, as well the work of [44, 45] on as spatial structure of galaxies.

Stable/unstable manifolds appear commonly in the geometric theory of dynamical sys-

tems as seperatrices or transport barriers. We refer for example to the work of [46, 47, 48] on generalizations of Melnikov theory based on the study of stable/manifolds and their intersections. Numerical methods for computing connecting orbits are often based on the idea of solving a boundary value problem for orbits beginning on an unstable and terminating on a stable manifold. See for example the general numerical methods developed in [49, 50, 51] and also the lecture notes [52]. We also refer the interested reader to the works of [14, 12, 11] for discussion of numerical methods which combine high order parameterization of the local stable/unstable manifolds with shooting methods for solving discrete time boundary value problems in order to compute connecting orbits for maps.

Of course, the references mentioned in this section barely scratch the surface of the relevant literature. The discussion above is only meant to provide some motivation and context for the present work within the existing literature.

3 A Parameterization Method for Periodic Orbits

Let $f\colon \mathbb{R}^M \to \mathbb{R}^M$ be a diffeomorphism and recall that f^N denotes the composition of the map f with itself N times (let f^0 be the identity map). A period N point for the map f is a $p \in \mathbb{R}^M$ so that

$$f^N(p) = p,$$

i.e. p is a fixed point of the map f^N. We say that the point p is a hyperbolic period N point for f if p is a hyperbolic fixed point of f^N, i.e. if the matrix $Df^N(p)$ has no eigenvalues on the unit circle. We say that p has least period N if

$$f^j(p) \neq f^k(p), \qquad \text{for } 1 \leq j \neq k \leq N.$$

In both numerical and theoretical considerations of period N points it is often useful to consider the following "multiple shooting" scheme. We introduce the variables $p = p_1$, and $f(p_j) = p_{j+1}$ for $j \geq 1$ and look for solutions of the following system of equations

$$\begin{aligned} f(p_1) &= p_2 \\ f(p_2) &= p_3 \\ &\vdots \\ f(p_N) &= p_1 \end{aligned}$$

We refer to $p_1, \ldots, p_N$ as a periodic orbit for f. Motivated by this system of equations we define also the mapping $F\colon \mathbb{R}^{M\times N} \to \mathbb{R}^{M\times N}$ by

$$F(p_1, \ldots, p_N) = \begin{pmatrix} f(p_N) \\ f(p_1) \\ \vdots \\ f(p_{N-1}) \end{pmatrix}. \tag{6}$$

and note that if $(p_1, \ldots, p_N) \in \mathbb{R}^{M\times N}$ is is a fixed point if F then any of the points p_j, $1 \leq j \leq N$ is a period N point for f. Moreover if $p_i \neq p_j$ for $i \neq j$ then each of the p_j, $1 \leq j \leq N$ has least period N.

Note that the differential of F is given by

$$DF(p_1,\dots,p_N) = \begin{pmatrix} 0 & 0 & \dots & 0 & Df(p_N) \\ Df(p_1) & 0 & \dots & 0 & 0 \\ 0 & Df(p_2) & \dots & 0 & 0 \\ \vdots & \vdots & \ddots & \vdots & \vdots \\ 0 & 0 & \dots & Df(p_{N-1}) & 0 \end{pmatrix}.$$

Moreover suppose that $\mathbf{p} = (p_1,\dots,p_N) \in \mathbb{R}^{M\times N}$ is a fixed point of F, and let $\lambda \in \mathbb{C}$ and $\xi = (\xi_1,\dots,\xi_N) \in \mathbb{R}^{M\times N}$. Then we have the following proposition.

Proposition 3.1. *Suppose that $\mathbf{p} \in \mathbb{R}^{MN}$ is a fixed point of F. Then λ, ξ is an eigenvalue/eigenvector pair for $DF(\mathbf{p})$ if and only if for each $1 \le j \le N$, $\sqrt[N]{\lambda}, \xi_j$ is an eigenvalue/eigenvector pair for $Df^N(p_j)$.*

Proof. Note that $\lambda \neq 0$ as f is a diffeomorphism. Moreover each of the matrices $Df(p_j)$ is invertible. Starting with $DF(\mathbf{p})\xi = \lambda\xi$ and rewriting it as the system:

$$\begin{aligned} Df(p_N)\xi_N &= \lambda\xi_1 \\ Df(p_1)\xi_1 &= \lambda\xi_2 \\ &\vdots \\ Df(p_{N-1})\xi_{N-1} &= \lambda\xi_{N-1} \end{aligned}$$

we get that:

$$\begin{aligned} Df(p_{j+1})Df(p_j)\xi_j &= \lambda^2\xi_{j+2} \\ &\vdots \\ Df(p_{j-1})\cdots Df(p_1)Df(p_N)\cdots Df(p_j)\xi_j &= \lambda^N\xi_j \end{aligned}$$

i.e $Df^N(p_j)\xi_j = \lambda^N\xi_j$, by the chain rule. Reversing the computation gives the reverse implication.

□

The proposition says that we recover the stability of each of the period N points p_j, $1 \le j \le N$ by computing the stability of the fixed point $\mathbf{p}$. Note that the proof also recovers the classic fact that if $p_1,\dots,p_N$ is a periodic orbit of least period N then each of the periodic points has the same eigenvalues. Moreover, the periodic orbit is hyperbolic if and only if $\mathbf{p}$ is a hyperbolic fixed point.

3.1 Composition free invariance equations

Continuing the notation established in Section 3, let $p_1,\dots,p_N \in \mathbb{R}^M$ be a hyperbolic periodic orbit of the smooth map $f\colon \mathbb{R}^M \to \mathbb{R}^M$, and let $\tilde{\lambda}_1,\dots,\tilde{\lambda}_m$ denote the stable eigenvalues of any of the matrices $Df^N(p_j)$, $1 \le j \le N$ (as each of these matrices has the same eigenvalues). Assume that $Df^N(p)$ is diagonalizable and let $\tilde{\xi}_1,\dots,\tilde{\xi}_m$ denote a linearly independent choice of eigenvectors. Motivated by the above considerations for periodic points we develop a "multiple shooting" approach to the parameterization of stable/unstable manifolds for a period N point. Let

$$\lambda_j := \left(\tilde{\lambda}_j\right)^{\frac{1}{N}},$$

for each $1 \leq j \leq m$.

Our goal is to find smooth functions $P^{(j)}\colon B_1^m(0) \to \mathbb{R}^M$, $1 \leq j \leq N$ which satisfy the first order constraints

$$P^{(j)}(0) = p_j, \qquad \text{and} \qquad \frac{\partial}{\partial \theta_k} P^{(j)}(0) = \xi_k^{(j)}, \tag{7}$$

for $1 \leq j \leq N$ and $1 \leq k \leq m$, and solve the system of invariance equations

$$\begin{array}{rcl} f\left(P^{(1)}\left(\theta_1, \ldots, \theta_m\right)\right) & = & P^{(2)}\left(\lambda_1\theta_1, \ldots, \lambda_m\theta_m\right) \\ f\left(P^{(2)}\left(\theta_1, \ldots, \theta_m\right)\right) & = & P^{(3)}\left(\lambda_1\theta_1, \ldots, \lambda_m\theta_m\right) \\ & \vdots & \\ f\left(P^{(N-1)}\left(\theta_1, \ldots, \theta_m\right)\right) & = & P^{(N)}\left(\lambda_1\theta_1, \ldots, \lambda_m\theta_m\right) \\ f\left(P^{(N)}\left(\theta_1, \ldots, \theta_m\right)\right) & = & P^{(1)}\left(\lambda_1\theta_1, \ldots, \lambda_m\theta_m\right), \end{array} \tag{8}$$

for $\theta_1, \ldots, \theta_m \in B_1^m(0)$.

The following discussion explains our interest in this system. Suppose that $\left(P^{(1)}, \ldots, P^{(N)}(\theta)\right)$ is a solution of the system of Equations (8). Then

$$f[P^{(1)}(\theta_1, \ldots, \theta_m)] = P^{(2)}(\lambda_1\theta_1, \ldots, \lambda_m\theta_m)$$

so that

$$f\left(f[P^{(1)}(\theta_1, \ldots, \theta_m)]\right) = f[P^{(2)}(\lambda_1\theta_1, \ldots, \lambda_m\theta_m)] = P^{(3)}(\lambda_1^2\theta_1, \ldots, \lambda_m^2\theta_m),$$

or

$$f^2[P^{(1)}(\theta_1, \ldots, \theta_m)] = P^{(3)}(\lambda_1^2\theta_1, \ldots, \lambda_m^2\theta_m).$$

Proceeding in this way leads to

$$f^k[P^{(1)}(\theta_1, \ldots, \theta_m)] = P^{(k+1)}(\lambda_1^k\theta_1, \ldots, \lambda_m^k\theta_m),$$

for $1 \leq k \leq N-1$ and finally

$$f^N[P^{(1)}(\theta_1, \ldots, \theta_m)] = P^{(1)}(\lambda_1^N\theta_1, \ldots, \lambda_m^N\theta_m),$$

which is

$$f^N[P^{(1)}(\theta_1, \ldots, \theta_m)] = P^{(1)}(\tilde{\lambda}_1\theta_1, \ldots, \tilde{\lambda}_m\theta_m).$$

so that $P^{(1)}$ satisfies the parameterization conjugacy equation for the composition map f^N. Repeating this computation for each $P^{(k)}$ with $2 \leq k \leq N$ gives the following.

Claim 1: If $P(\theta) := (P^1(\theta_1, \ldots, \theta_m), \ldots, P^{(N)}(\theta_1, \ldots, \theta_m))$ solves the system of equations given by (8), then $P^{(k)}$ parameterizes the local stable manifold at p_k for each $1 \leq k \leq N$.

In order to solve the system of invariance equations we consider the case that f is analytic and look for formal series solutions

$$P^{(k)}(\theta_1, \ldots, \theta_m) = \sum_{|\alpha|=0}^{\infty} p_\alpha^{(k)}\theta^\alpha,$$

or

$$P(\theta) = \sum_{|\alpha|=0}^{\infty} p_\alpha\theta^\alpha, \qquad \text{where} \qquad p_\alpha = \begin{pmatrix} p_\alpha^{(1)} \\ \vdots \\ p_\alpha^{(N)} \end{pmatrix}.$$

We will see that if $F\colon \mathbb{R}^{MN} \to \mathbb{R}^{MN}$ is the map defined in Equation (6), and if $p = (p_1, \ldots, p^N) \in \mathbb{R}^{MN}$ denotes the periodic orbit then the coefficients of P solve homological equations of the form

$$[DF(p) - \lambda_1^{\alpha_1} \ldots \lambda_m^{\alpha_m} \mathrm{Id}_{\mathbb{R}^{MN}}]\, p_\alpha = S_\alpha. \tag{9}$$

Here S_α is a nonlinear function of the coefficients $\{p_\beta\}$ with $|\beta| < \alpha$, and form of the nonlinearity of S_α depends only on the nonlinearity of f (rather than the nonlinearity f^N). Deriving the explicit form of S_α is a problem dependent question best illustrated in specific examples.

Note that

$$\lambda_1^{\alpha_1} \ldots \lambda_m^{\alpha_m} = \lambda_k,$$

for some $1 \le k \le N$ and some fixed multi-index $(\alpha_1, \ldots, \alpha_m) \in \mathbb{Z}^m$ if and only if

$$\tilde{\lambda}_1^{\alpha_1} \ldots \tilde{\lambda}_m^{\alpha_m} = \tilde{\lambda}_k,$$

with the same data, i.e. the homological Equations (9) have unique solution p_α for each $\alpha \in \mathbb{N}^m$ if and only if the eigenvalues of $Df^N(p_k)$ are non-resonant. Then the "multiple-shooting" version of the Parameterization method is applicable if and only if the standard version applies to the fixed point of the composition map.

Claim 2: (real analytic parameterizations:) by choosing appropriately the eigenvectors, we can always arrange that the image of the parameterizations are real. Starting with a real eigenvalue and eigenvector of $Df^N(p_j)$, call it ${u_1}^{[j]}$, it is easy to see from the recursive equation $(Df^N(p_j) - \lambda^{Nn} I){u_\alpha}^{[j]} = {S'_\alpha}^{[j]}$ that ${u_n}^{[j]}$ is real for all n. Now we rewrite $(DF(p_*) - \lambda^n I)u_\alpha = S_\alpha$ as a system using block multiplication, i.e.

$$Df(p_N){u_\alpha}^{[N]} - \lambda^\alpha {u_\alpha}^{[1]} = {S_\alpha}^{[1]},$$

and

$$Df(p_j){u_\alpha}^{[j]} - \lambda^\alpha {u_\alpha}^{[j+1]} = {S_\alpha}^{[j+1]},$$

for $j = 1, \cdots, N-1$. This system leads to

$$(Df(p_{j-1}) \cdots Df(p_1) Df(p_N) \cdots Df(p_j) - \lambda^{N\alpha} I){u_\alpha}^{[j]} = \Sigma_\alpha^{[j]},$$

i.e.

$$(Df^N(p_j) - \lambda^{N\alpha} I){u_\alpha}^{[j]} = \Sigma_\alpha^{[j]},$$

where

$$\begin{aligned} \Sigma_\alpha^{[j]} &= (Df(p_j) \cdots Df(p_1) Df(p_N) \cdots Df(p_{j+1})){S_\alpha}^{[j]} \\ &+ \lambda^\alpha (Df(p_j) \cdots Df(p_1) Df(p_N) \cdots Df(p_{j+2})){S_\alpha}^{[j+1]} \\ &+ \cdots \\ &+ \lambda^{(N-1)\alpha} {S_\alpha}^{[j-1]}, \end{aligned}$$

i.e

$$\Sigma_\alpha^{[j]} = Df^N(p_{j+1}){S_\alpha}^{[j]} + \lambda^\alpha Df^{N-1}(p_{j+2}){S_\alpha}^{[j+1]} + \cdots + \lambda^{(N-1)\alpha}{S_\alpha}^{[j-1]}[*].$$

Now $(Df^N(p_j) - \lambda^{N\alpha} I)$ is a real matrix and hence it is enough to assure that $\Sigma_\alpha^{[j]}$ is real.

For $\Sigma_\alpha^{[j]}$ a finite sum of convolution terms then the above suggests to multiply ${u_1}^{[j-1]}$ by $\lambda \cdots$ and ${u_1}^{[j+1]}$ by λ^{N-1} . In practice we multiply ${u_1}^{[j-1]}$ by a primitive N root of

unity $\alpha \cdots$ and ${u_1}^{[j+1]}$ by α^{N-1}. Using automatic differentiation the argument extends to non-polynomial nonlinearities as well.

For simplicity of the argument pick ${u_1}^{[N]}$ real, then using induction on [*] we show that ${u_n}^{[j]}\lambda^{N-j}$ is real for all n and j and it also shows that multiplying ${u_1}^{[j]}$ by λ and recomputing ${u_n}^{[j]}$ to evaluate $P'^{[j]}(\theta)$ is equivalent to computing $P^{[j]}(\lambda\theta)$.

Claim 3: (Non-uniqueness and scaling the eigenvectors:) by choosing appropriately the scalings of the eigenvectors we can arrange that the Taylor series coefficients of the parameterizations have whatever exponential decay rate we like.

To see this note that Lemma 2.5 tells us that solutions of Equation (4) are unique up to the choice of the scalings of the eigenvectors at the fixed point. The same follows for the system given by Equation (8), precisely because solutions of the system of Equations (8) are equivalent to solutions of Equation (4) for the composition map.

Moreover we can work out exactly the effect of rescaling the eigenvectors on the Taylor coefficients of the solution. To this end consider

$$P^{(k)}(\theta_1, \ldots, \theta_m) = \sum_{|\alpha|=0}^{\infty} p_\alpha^{(k)} \theta^\alpha,$$

for $1 \leq k \leq m$ solving the system of Equations (8), and suppose that the eigenvectors $\xi_j = (p_{e_j}^{(1)}, \ldots, p_{e_j}^{(N)})$ hase $\|\xi_j\| = 1$. Now choose scalings $0 < \sigma_j$ for $1 \leq j \leq m$ and define the vector $\sigma = (\sigma_1, \ldots, \sigma_m)$, as well as the new collection of functions

$$\hat{P}^{(k)}(\theta_1, \ldots, \theta_m) = \sum_{|\alpha|=0}^{\infty} \hat{p}_\alpha^{(k)} \theta^\alpha,$$

where

$$\hat{p}_\alpha^{(k)} = \sigma^\alpha p_\alpha^{(k)}, \qquad 1 \leq k \leq m. \tag{10}$$

Note that

$$\hat{p}_0^{(k)} = \sigma^0 p_0^{(k)} = p_k,$$

and

$$\hat{p}_{e_j}^{(k)} = \sigma^{e_j} p_0^{(k)} = \sigma_j p_{e_j}^{(k)},$$

i.e. $\hat{P}$ satisfies the first order constraints given by Equation (7).

Now define the new variables

$$\hat{\theta}_j = \frac{\theta_j}{\sigma_j},$$

for $1 \leq j \leq m$. Then

$$\begin{aligned}
\hat{P}^{(k)}(\hat{\theta}_1, \ldots, \hat{\theta}_m) &= \sum_{|\alpha|=0}^{\infty} \hat{p}_\alpha^{(k)} \hat{\theta}^\alpha \\
&= \sum_{|\alpha|=0}^{\infty} \sigma^\alpha p_\alpha^{(k)} \hat{\theta}^\alpha \\
&= \sum_{|\alpha|=0}^{\infty} p_\alpha^{(k)} \theta^\alpha \\
&= P^{(k)}(\theta_1, \ldots, \theta_m).
\end{aligned}$$

Then

$$\begin{aligned} P^{(k)}(\lambda_1\theta_1, \ldots, \lambda_m\theta_m) &= f[P^{(k+1)}(\theta_1, \ldots, \theta_m)] \\ &= f[\hat{P}^{(k+1)}(\hat{\theta}_1, \ldots, \hat{\theta}_m)]. \end{aligned}$$

Combining these observations gives that

$$f[\hat{P}^{(k+1)}(\hat{\theta}_1, \ldots, \hat{\theta}_m)] = \hat{P}^{(k)}(\lambda_1\hat{\theta}_1, \ldots, \lambda_m\hat{\theta}_m),$$

i.e. that $\hat{P}$ is the solution of the system given by Equation (8), subject to the linear constraints with eigenvectors scaled by σ. By uniqueness $\hat{P}$ is the only such solution. This shows that given one solution of Equation (8) whose Taylor coefficients are $\{p_\alpha\}$, rescaling the eigenvectors by σ leads to a new solution of Equation (8) whose Taylor coefficients are determined from $\{p_\alpha\}$ by Equation (10).

3.2 Formal solution of the invariance equations

We now study the system of invariance equations (8) for a number of particular example problems. Our goal is to illustrate the derivation of the homological equations which are essential for implementing the Parameterization Method numerically.

3.2.1 A worked example: parameterization of stable/unstable manifolds for saddle type period 2 orbits for the Henon Map

As a simple example is to consider the stable manifold attached to a hyperbolic period of the Henon map [53]. The Henon map $f\colon \mathbb{R}^2 \to \mathbb{R}^2$ is the quadratic polynomial diffeomorphism of the plane given by

$$f(x, y) = \begin{pmatrix} 1 + y - ax^2 \\ bx \end{pmatrix}, \tag{11}$$

with $a, b \in \mathbb{R}$. The map is invertible with quadratic inverse.

Suppose that $p_0, q_0 \in \mathbb{R}^2$ is a saddle type period 2 orbit for f, i.e. that

$$f(p_0) = q_0, \qquad \text{and} \qquad f(q_0) = p_0,$$

with $p_0 \neq q_0$, that $\tilde{\lambda} \in \mathbb{R}$ has $|\tilde{\lambda}| < 1$, and $\xi, \eta \in \mathbb{R}^2$ have that

$$Df^2(p_0)\xi = \tilde{\lambda}\xi, \qquad \text{and} \qquad Df^2(q_0)\eta = \tilde{\lambda}\eta,$$

and that the remaining eigenvalue of $Df^2(p_0)$, $Df^2(q_0)$ is unstable. Define

$$\lambda = \sqrt{\tilde{\lambda}}.$$

In this setting the system of invariance equations given by Equation (8) reduces to

$$\begin{aligned} f(Q(\theta)) &= P(\lambda\theta) \\ f(P(\theta)) &= Q(\lambda\theta) \end{aligned}. \tag{12}$$

We look for P, Q of the form

$$P(\theta) = \sum_{n=0}^{\infty} p_n\theta^n,$$

and

$$Q(\theta) = \sum_{n=0}^{\infty} q_n \theta^n,$$

require that

$$P(0) = p_0, \qquad \text{and} \qquad Q(0) = q_0,$$

(so that q_0, p_0 denote the zero-th Taylor coefficient as well as the periodic orbit), and also that

$$P'(0) = p_1 = \xi, \qquad \text{and} \qquad Q'(0) = q_1 = \eta,$$

so that P and Q are tangent to the correct eigenspaces.

We will derive the explicit form of the homological equation (9). To this end note that

$$P(\lambda\theta) = \sum_{n=0}^{\infty} \lambda^n p_n \theta^n, \qquad \text{and} \qquad Q(\lambda\theta) = \sum_{n=0}^{\infty} \lambda^n q_n \theta.$$

Writing

$$p_n = \begin{pmatrix} p_n^1 \\ p_n^2 \end{pmatrix}, \qquad \text{and} \qquad q_n = \begin{pmatrix} q_n^1 \\ q_n^2 \end{pmatrix},$$

for the components of the Taylor coefficients, and employing the Cauchy product for power series, we have

$$f(P(\theta)) = \begin{pmatrix} 1 + \sum_{n=0}^{\infty} p_n^2 - \sum_{n=0}^{\infty} \sum_{k=0}^{n} a p_{n-k}^1 p_k^1 \\ \sum_{n=0}^{\infty} b p_n^1 \end{pmatrix},$$

and

$$f(Q(\theta)) = \begin{pmatrix} 1 + \sum_{n=0}^{\infty} q_n^2 - \sum_{n=0}^{\infty} \sum_{k=0}^{n} a q_{n-k}^1 q_k^1 \\ \sum_{n=0}^{\infty} b q_n^1 \end{pmatrix},$$

Plugging these power series expansions into Equation (12) and matching like powers of θ for $n \geq 2$ leads to

$$\begin{pmatrix} q_n^2 - \sum_{k=0}^{n} a q_{n-k}^1 q_k^1 \\ b q_n^1 \\ p_n^2 - \sum_{k=0}^{n} a p_{n-k}^1 p_k^1 \\ b p_n^1 \end{pmatrix} = \begin{pmatrix} \lambda^n p_n^1 \\ \lambda^n p_n^2 \\ \lambda^n q_n^1 \\ \lambda^n q_n^2 \end{pmatrix}$$

or

$$\begin{pmatrix} q_n^2 - 2a q_0^1 q_n^1 - \sum_{k=1}^{n-1} a q_{n-k}^1 q_k^1 \\ b q_n^1 \\ p_n^2 - 2a p_0^1 p_n^1 - \sum_{k=1}^{n-1} a p_{n-k}^1 p_k^1 \\ b p_n^1 \end{pmatrix} = \lambda^n \begin{pmatrix} p_n^1 \\ p_n^2 \\ q_n^1 \\ q_n^2 \end{pmatrix}.$$

Moving terms of order n to the left, terms of lower order to the right, and observing that the dependance on p_n, q_n is linear leads to

$$\left[\begin{pmatrix} 0 & 0 & -2aq_0^1 & 1 \\ 0 & 0 & b & 0 \\ -2p_0^1 & 1 & 0 & 0 \\ b & 0 & 0 & 0 \end{pmatrix} - \lambda^n \begin{pmatrix} 1 & 0 & 0 & 0 \\ 0 & 1 & 0 & 0 \\ 0 & 0 & 1 & 0 \\ 0 & 0 & 0 & 1 \end{pmatrix} \right] \begin{bmatrix} p_n^1 \\ p_n^2 \\ q_n^1 \\ q_n^2 \end{bmatrix} = \begin{bmatrix} a \sum_{k=1}^{n-1} q_{n-k}^1 q_k^1 \\ 0 \\ a \sum_{k=1}^{n-1} p_{n-k}^1 p_k^1 \\ 0 \end{bmatrix}. \tag{13}$$

Letting $F\colon \mathbb{R}^2 \to \mathbb{R}^4$ be the map

$$F(p,q) = \begin{pmatrix} 1 + q_2 - aq_1^2 \\ bq_1 \\ 1 + p_2 - ap_1^2 \\ bp_1 \end{pmatrix},$$

we see that indeed Equation (13) has exactly the form promised in Equation (9). The point of working through the computation above is that we now know explicitly the form of the right hand side of the homological equation, and this knowledge is used to implement numerical algorithms.

Note that for all $n \geq 2$, λ^n is not an eigenvalue of $DF(p_0, q_0)$. This is because we assumed that p_0, q_0 is a hyperbolic saddle, hence the only other eigenvalue has absolute value greater than one. Then $|\lambda^n| < |\lambda| < 1$ for all $n \geq 2$, hence λ^n is never an eigenvalue. Equation (13) is characteristic for $DF(p_0, q_0)$, and we have that solutions exist and are unique for any right hand side and for as long $n \geq 2$. This is a specific instance of a more general result: namely that a saddle with exactly one stable eigenvalue is never resonant. Solving Equation (13) recursively for each $2 \leq n \leq K$ leads to the polynomial approximations

$$P^K(\theta) = \sum_{n=0}^{K} p_n \theta^n, \qquad \text{and} \qquad Q^K(\theta) = \sum_{n=0}^{K} q_n \theta^n.$$

Also note that if we consider instead the unstable eigenvalues all of the comments above go through. We discuss numerical methods further in Section 4.

3.2.2 The homological equations for a period N point of Henon

Suppose now that $p^1, \ldots, p^N \in \mathbb{R}^2$ is a periodic orbit of the Hénon map with least period N, and that $\tilde{\lambda} \in \mathbb{R}$ and $\xi^1, \ldots, \xi^N \in \mathbb{R}^2$ have that

$$Df^N(p^k)\xi^k = \tilde{\lambda}\xi^k,$$

for $1 \leq k \leq N$. Define the map

$$F(x_1, y_1, x_2, y_2, \ldots, x_N, y_N) = \begin{pmatrix} 1 + y_N - ax_N^2 \\ bx_N \\ 1 + y_2 - ax_2^2 \\ bx_2 \\ \vdots \\ 1 + y_1 - ax_1^2 \\ bx_1 \end{pmatrix}.$$

Define

$$\lambda = \sqrt[N]{\tilde{\lambda}}.$$

Note that $p^1, \ldots, p^N$ is a fixed point of F and that $\tilde{\lambda}$, $\xi^1, \ldots, \xi^N$ can be computed by finding eigenvalues/eigenvectors for $DF(p^1, \ldots, p^N)$.

Let $p_0, p_1 \in \mathbb{R}^{2N}$ be

$$p_0 = \begin{pmatrix} p^1 \\ \vdots \\ p^N \end{pmatrix}, \qquad \text{and} \qquad p_1 = \begin{pmatrix} \xi^1 \\ \vdots \\ \xi^N \end{pmatrix}.$$

We seek

$$P(\theta) = \begin{pmatrix} P^{(1)}(\theta) \\ \vdots \\ P^{(N)}(\theta) \end{pmatrix},$$

solving the invariance equation, with

$$P^{(k)}(\theta) = \sum_{n=0}^{\infty} p_n^k \theta^n,$$

for $p_n^k \in \mathbb{R}^2$ for $1 \leq k \leq N$. We write $p_n^k = (p_{n,1}^k, p_{n,2}^k)$ to denote the components. Define $p_n \in \mathbb{R}^{2N}$ by

$$p_n = \begin{pmatrix} p_n^1 \\ \vdots \\ p_n^N \end{pmatrix}.$$

A computation similar to that illustrated in detail in Section 3.2.1 shows that each $p_n \in \mathbb{R}^{2N}$ with $n \geq 2$ is a solution of the equation

$$[DF(p_0) - \lambda^n \mathrm{Id}_{2N\times 2N}]\, p_n = s_n^N,$$

with s_n^N defined by

$$s_n^N := \begin{pmatrix} a\sum_{k=1}^{n-1} p_{n-k,1}^N p_{k,1}^N \\ 0 \\ a\sum_{k=1}^{n-1} p_{n-k,1}^2 p_{k,1}^2 \\ 0 \\ \vdots \\ a\sum_{k=1}^{n-1} p_{n-k,1}^{N-1} p_{k,1}^{N-1} \\ 0 \\ a\sum_{k=1}^{n-1} p_{n-k,1}^1 p_{k,1}^1 \\ 0 \end{pmatrix}.$$

Again, we see that the linear system has unique solution for all $n \geq 2$ by the assumption that the orbit is hyperbolic, as $\lambda^n \neq \lambda$ for any $n \geq 2$. Solving the system to order K leads to the polynomial approximation

$$P_K(\theta) := \sum_{n=0}^{K} p_n \theta^n.$$

3.2.3 Example of a two dimensional manifold for a three dimensional map: stable/unstable manifolds for periodic orbits of the Lomelí Map

Consider the map $f\colon \mathbb{R}^3 \to \mathbb{R}^3$ given by

$$f(x,y,z) = \begin{pmatrix} z + Q(x,y) \\ x \\ y \end{pmatrix} \tag{14}$$

where Q is the quadratic form

$$Q(x,y) = \alpha + \tau x + ax^2 + bxy + cy^2.$$

We refer to Equation (14) as the Lomelí map. It is standard to choose parameters normalized so that $a+b+c=1$. The Lomelí map is a normal form for quadratic volume preserving maps with quadratic inverse. In that sense it can be thought of as a three dimensional generalization of the planar Hénon map. The dynamics of the Lomelí map are considered in a number of studies, see for example [54, 55, 56, 12].

Now let

$$F(x_1,y_1,z_1,\ldots,x_N,y_N,z_N)=\begin{pmatrix} z_N+Q(x_N,y_N)\\ x_N\\ y_N\\ \vdots\\ z_1+Q(x_1,y_1)\\ x_1\\ y_1\end{pmatrix}.$$

Suppose that $(p^1,\ldots,p^N)\in\mathbb{R}^{3N}$ is a fixed point of F, i.e. $p^1,\ldots,p^N$ is a periodic orbit.

We focus on the case that the orbit is hyperbolic with a complex conjugate pair of stable/unstable eigenvalues. More precisely, assume that $Df^N(p_k)$ has a complex conjugate pair of eigenvalues $\tilde{\lambda},\overline{\tilde{\lambda}}\in\mathbb{C}$ and let $\xi^k,\bar{\xi}^k$ be an associated choice of complex conjugate eigenvectors. We choose λ, and $\bar{\lambda}$ to be complex conjugates with

$$\lambda=\sqrt[N]{\tilde{\lambda}},\qquad\text{and}\qquad\bar{\lambda}=\sqrt[N]{\overline{\tilde{\lambda}}}.$$

Of course we have again that $\lambda,\bar{\lambda},\ \xi^1,\bar{\xi}^1,\ldots,\xi^N,\bar{\xi}^N$ can be found by computing eigenvalues/eigenvectors of $DF(p^1,\ldots,p^N)$.

In this case we employ complex variables and look for $P^{(k)}\colon\mathbb{C}^2\to\mathbb{C}^3$ solving the invariance equations

$$\begin{aligned} f(P^{(N)}(z_1,z_2)) &= P^{(1)}(\lambda z_1,\bar{\lambda}z_2)\\ f(P^{(1)}(z_1,z_2)) &= P^{(2)}(\lambda z_1,\bar{\lambda}z_2)\\ &\vdots\\ f(P^{(N-1)}(z_1,z_2)) &= P^{(N)}(\lambda z_1,\bar{\lambda}z_2).\end{aligned}$$

We look for solutions in the form

$$P^{(k)}(z_1,z_2)=\sum_{n_1=0}^{\infty}\sum_{n_2=0}^{\infty}p^k_{n_1,n_2}z_1^{n_1}z_2^{n_2},$$

for each $1\le k\le N$ where $p^k_{n_1,n_2}\in\mathbb{C}^3$ for each $n_1,n_2\in\mathbb{N}$. We express the components as $p^k_{n_1,n_2}=(p^k_{n_1,n_2,1},p^k_{n_1,n_2,2},p^k_{n_1,n_2,3})\in\mathbb{C}^3$. We write

$$p_0=\begin{pmatrix}p^1\\ \vdots\\ p^N\end{pmatrix},\qquad p_{0,1}=\begin{pmatrix}\xi^1\\ \vdots\\ \xi^N\end{pmatrix}\qquad\text{and}\qquad p_{1,0}=\begin{pmatrix}\bar{\xi}^1\\ \vdots\\ \bar{\xi}^N\end{pmatrix},$$

for the zero and first order Taylor coefficients, and more generally

$$P(z_1,z_2)=\sum_{n_1=0}^{\infty}\sum_{n_2=0}^{\infty}p_{n_1,n_2}z_1^{n_1}z_2^{n_2},$$

where

$$p_{n_1,n_2} = \begin{pmatrix} p^1_{n_1,n_2} \\ \vdots \\ p^N_{n_1,n_2} \end{pmatrix}.$$

Noting that

$$P^{(k)}(\lambda z_1, \bar{\lambda} z_2) = \sum_{n_1=0}^{\infty} \sum_{n_2=0}^{\infty} \lambda^{n_1} \bar{\lambda}^{n_2} p^{(k)}_{n_1,n_2} z_1^{n_1} z_2^{n_2},$$

and (after using the two variable Cauchy product) that

$$f[P^{(k)}(z_1, z_2)] =$$

$$= \begin{pmatrix} \alpha + \sum_{n_1=0}^{\infty} \sum_{n_2=0} \infty \left(p^{(k)}_{n_1,n_2,3} + \tau p^{(k)}_{n_1,n_2,1} + q^{(k)}_{n_1,n_2} \right) z_1^{n_1} z_2^{n_2} \\ \sum_{n_1=0}^{\infty} \sum_{n_2=0}^{\infty} p^{(k)}_{n_1,n_2,1} z_1^{n_1} z_2^{n_2} \\ \sum_{n_1=0}^{\infty} \sum_{n_2=0}^{\infty} p^{(k)}_{n_1,n_2,2} z_1^{n_1} z_2^{n_2} \end{pmatrix}$$

where

$$q^{(k)}_{n_1,n_2} = \sum_{i=0}^{n_1} \sum_{j=0}^{n_2} a p^{(k)}_{n_1-i,n_2-j,1} p^{(k)}_{i,j,1} + b p^{(k)}_{n_1-i,n_2-j,1} p^{(k)}_{i,j,2} + c p^{(k)}_{n_1-i,n_2-j,2} p^{(k)}_{i,j,2}.$$

Matching like powers for $n_1 + n_2 \geq 2$ leads to

$$\begin{pmatrix} p^{(N)}_{n_1,n_2,3} + \tau p^{(N)}_{n_1,n_2,1} + q^{(N)}_{n_1,n_2} \\ p^{(N)}_{n_1,n_2,1} \\ p^{(N)}_{n_1,n_2,2} \end{pmatrix} = \lambda^{n_1} \bar{\lambda}^{n_2} \begin{pmatrix} p^{(1)}_{n_1,n_2,1} \\ p^{(1)}_{n_1,n_2,2} \\ p^{(1)}_{n_1,n_2,3} \end{pmatrix}$$

and

$$\begin{pmatrix} p^{(k-1)}_{n_1,n_2,3} + \tau p^{(k-1)}_{n_1,n_2,1} + q^{(k-1)}_{n_1,n_2} \\ p^{(k-1)}_{n_1,n_2,1} \\ p^{(k-1)}_{n_1,n_2,2} \end{pmatrix} = \lambda^{n_1} \bar{\lambda}^{n_2} \begin{pmatrix} p^{(k)}_{n_1,n_2,1} \\ p^{(k)}_{n_1,n_2,2} \\ p^{(k)}_{n_1,n_2,3} \end{pmatrix}$$

for $2 \leq k \leq N$. Let $s_{n_1,n_2} = (s^{(N)}_{n_1,n_2}, s^{(1)}_{n_1,n_2}, \ldots, s^{(N-1)}_{n_1,n_2})$ and

$$s^{(k)}_{n_1,n_2} = \begin{pmatrix} \sum_{i=0}^{n_1} \sum_{j=0}^{n_2} \delta^{n_1,n_2}_{j,k} \left(a p^{(k)}_{n_1-i,n_2-j,1} p^{(k)}_{i,j,1} + b p^{(k)}_{n_1-i,n_2-j,1} p^{(k)}_{i,j,2} + c p^{(k)}_{n_1-i,n_2-j,2} p^{(k)}_{i,j,2} \right) \\ 0 \\ 0 \end{pmatrix}, \tag{15}$$

where we define

$$\delta^{n_1,n_2}_{j,k} := \begin{cases} 0 & \text{if } j = n_1 \text{ and } k = n_2 \\ 0 & \text{if } j = 0 \text{ and } k = 0 \\ 1 & \text{otherwise} \end{cases}.$$

Then

$$q^{(k)}_{n_1,n_2} = 2a p^{(k)}_{0,0,1} p_{n_1,n_2,1} + b p_{0,0,1} p_{n_1,n_2,2} + b p_{0,0,2} p_{n_1,n_2,1} + c p_{0,0,2} p_{n_1,n_2,2}$$

So, the Taylor coefficient p_{n_1,n_2} is found by solving the homological equation

$$\left[DF(p_0) - \lambda^{n_1} \bar{\lambda}^{n_2} \mathrm{Id}_{3N \times 3N} \right] p_{n_1,n_2} = s_{n_1,n_2}. \tag{16}$$

Again we remark that these are always uniquely solvable in the case under consideration, namely a periodic hyperbolic saddle with a complex conjugate pair. This is because if $n_1 + n_2 \geq 2$ then neither

$$\lambda^{n_1}\bar{\lambda}^{n_2} = \lambda \qquad \text{nor} \qquad \lambda^{n_1}\bar{\lambda}^{n_2} = \bar{\lambda},$$

are possible, and since the Lomelí map is volume preserving the third eigenvalue must have opposite stability from $\lambda, \bar{\lambda}$ (i.e. is unstable if they are stable or vice versa). More generally a periodic orbit with a single complex conjugate pair of stable (or unstable) eigenvalues cannot be resonant.

We write

$$P_K(\theta) = \sum_{n=0}^{K} \sum_{m=0}^{n} p_{n-mm} \theta_1^{n-m} \theta_2^m,$$

to denote the polynomial approximation obtained by solving the homological equations to order K.

Remark 3.2 (Real Parameterization)**.** In the end we are actually interested in the real dynamics of the Lomelí map, and want that the image if P is real. By Considering Equation (16) we see that solutions have the property

$$p_{m_2,m_1} = \overline{p_{m_1,m_2}}.$$

This complex conjugate property of the coefficients of P implies that if we choose complex conjugate variables

$$z_1 = \theta + i\phi, \qquad \text{and} \qquad z_2 = \theta - i\phi,$$

and define the polynomial

$$\hat{P}(\theta, \phi) = P(\theta + i\phi, \theta - i\phi),$$

where P has coefficients solving Equation (16), then $\hat{P}$ parameterizes the real local stable/unstable manifolds associated with the periodic orbit.

3.2.4 Example of a non-polynomial nonlinearity: automatic differentiation for the Standard Map

We now consider the map $f\colon \mathbb{R}^2 \to \mathbb{R}^2$ given by

$$f(x, y) = \begin{pmatrix} x + a\sin(y) \\ y + x + a\sin(y) \end{pmatrix}, \tag{17}$$

with $a \geq 0$. The map is known as *the standard map*, or as the Chirikov-Taylor map, and is widely studied as a toy model of symplectic dynamics [57, 58, 59]. For example the mapping exhibits dynamics similar to the dynamics of a Poincare section of a periodic orbit of a two freedom Hamiltonian system restricted to an energy surface. We now derive the homological equations for the parameterization of the stable/unstable manifold of a period N orbit of the standard map, in order to illustrate the use of our method for non-polynomial nonlinearities.

Then suppose that $p^1, \ldots, p^N \in \mathbb{R}^2$ are the points of a periodic orbit of least period N. Assume that the orbit is hyperbolic and let $\xi^1, \ldots, \xi^N \in \mathbb{R}^2$ and $\tilde{\lambda} \in \mathbb{R}$ denote the associated eigenvalues and eigenvectors. We let

$$\lambda = \sqrt[N]{\tilde{\lambda}},$$

and look for solutions

$$P^{(k)}(\theta) = \sum_{n=0}^{\infty} p_n^{(k)} \theta^n,$$

of Equation (8) in this setting. Let us write

$$p_n^{(k)} = \begin{pmatrix} p_{n,1}^{(k)} \\ p_{n,2}^{(k)} \end{pmatrix}$$

for $1 \leq k \leq N$, to denote the components of $p_n^{(k)}$.

This difference between the present case and the examples discussed above is that the Standard map has non-polynomial nonlinearity, so that evaluation of $f[P^{(k)}]$ cannot be evaluated simply using Cauchy products. Instead we employ a technique sometimes called *automatic differentiation for Taylor series*, or simply automatic differentation [60]. The idea is to exploit the fact that the sine and cosine functions are themselves solutions of simple differential equations.

In order to illustrate the idea we define for each $1 \leq k \leq N$ the functions $S^{(k)}, C^{(k)}$ by

$$S^{(k)}(\theta) := \sin\left(P_2^{(k)}(\theta)\right),$$

and

$$C^{(k)}(\theta) := \cos\left(P_2^{(k)}(\theta)\right),$$

and look for the Taylor series expansions

$$\sum_{n=0}^{\infty} s_n^{(k)} \theta^n = S^{(k)}(\theta),$$

and

$$\sum_{n=0}^{\infty} c_n^{(k)} \theta^n = C^{(k)}(\theta).$$

Taking derivatives we obtain

$$\frac{d}{d\theta} S^{(k)}(\theta) = \cos\left(P_2^{(k)}(\theta)\right) \frac{d}{d\theta} P_2^{(k)}(\theta),$$

and

$$\frac{d}{d\theta} C^{(k)}(\theta) = -\sin\left(P_2^{(k)}(\theta)\right) \frac{d}{d\theta} P_2^{(k)}(\theta),$$

which on the level of power series gives

$$\begin{aligned} \sum_{n=0}^{\infty} (n+1) s_{n+1}^{(k)} \theta^n &= \left(\sum_{n=0}^{\infty} c_n \theta^n\right) \left(\sum_{n=0}^{\infty} (n+1) p_{n,2}^{(k)} \theta^n\right) \\ &= \sum_{n=0}^{\infty} \sum_{j=0}^{n} (j+1) c_{n-j}^{(k)} p_{j+1,2}^{(k)} \theta^n \end{aligned}$$

and similarly

$$\sum_{n=0}^{\infty} (n+1) c_{n+1}^{(k)} \theta^n = -\sum_{n=0}^{\infty} \sum_{j=0}^{n} (j+1) s_{n-j}^{(k)} p_{j+1,2}^{(k)} \theta^n.$$

Of course we have that

$$s_0^{(k)} = \sin\left(p_{0,2}^{(k)}\right) \qquad \text{and} \qquad c_0^{(k)} = \cos\left(p_{0,2}^{(k)}\right),$$

as well as

$$s_1^{(k)} = \cos\left(p_{0,2}^{(k)}\right) p_{1,2}^{(k)} \qquad \text{and} \qquad c_1^{(k)} = -\sin\left(p_{0,2}^{(k)}\right) p_{1,2}^{(k)},$$

By matching like powers we obtain that

$$s_n^{(k)} = \frac{1}{n}\sum_{j=1}^{n} j c_{n-j}^{(k)} p_{j,2}^{(k)} = c_0^{(k)} p_{n,2}^{(k)} + \frac{1}{n}\sum_{j=1}^{n-1} j c_{n-j}^{(k)} p_{j,2}^{(k)},$$

and

$$c_n^{(k)} = \frac{-1}{n}\sum_{j=1}^{n} j s_{n-j}^{(k)} p_{j,2}^{(k)} = -s_0^{(k)} p_{j,2}^{(k)} - \frac{1}{n}\sum_{j=1}^{n-1} j s_{n-j}^{(k)} p_{j,2}^{(k)},$$

for $n \geq 2$.

Now let

$$P(\theta) = \begin{pmatrix} P^{(1)}(\theta) \\ \vdots \\ P^{(N)}(\theta) \end{pmatrix}$$

Then

$$P(\lambda\theta) = \sum_{n=0}^{\infty} \lambda^n p_n \theta^n,$$

while

$$\begin{aligned} f[P^{(k)}(\theta)] &= \begin{pmatrix} P_1^k(\theta) + a\sin\left(P_2^{(k)}(\theta)\right) \\ P_1^k(\theta) + P_2^{(k)}(\theta) + a\sin\left(P_2^{(k)}(\theta)\right) \end{pmatrix} \\ &= \sum_{n=0}^{\infty} \begin{pmatrix} p_{n,1}^{(k)} + a s_n^{(k)} \\ p_{n,1}^{(k)} + p_{n,2}^{(k)} + a s_n^{(k)} \end{pmatrix} \theta^n. \end{aligned}$$

The n-th coefficient of this power series is

$$\begin{aligned} \begin{pmatrix} p_{n,1}^{(k)} + a s_n^{(k)} \\ p_{n,1}^{(k)} + p_{n,2}^{(k)} + a s_n^{(k)} \end{pmatrix} &= \begin{pmatrix} p_{n,1}^{(k)} + a c_0^{(k)} p_{n,2}^{(k)} + \frac{a}{n}\sum_{j=1}^{n-1} j c_{n-j}^{(k)} p_{j,2}^{(k)}, \\ p_{n,1}^{(k)} + p_{n,2}^{(k)} + a c_0^{(k)} p_{n,2}^{(k)} + \frac{a}{n}\sum_{j=1}^{n-1} j c_{n-j}^{(k)} p_{j,2}^{(k)} \end{pmatrix} \\ &= \begin{pmatrix} 1 & a\cos\left(p_{0,2}^{(k)}\right) \\ 1 & 1 + a\cos\left(p_{0,2}^{(k)}\right) \end{pmatrix} \begin{bmatrix} p_{n,1}^{(k)} \\ p_{n,2}^{(k)} \end{bmatrix} + \begin{bmatrix} \frac{a}{n}\sum_{j=1}^{n-1} j c_{n-j}^{(k)} p_{j,2}^{(k)} \\ \frac{a}{n}\sum_{j=1}^{n-1} j c_{n-j}^{(k)} p_{j,2}^{(k)} \end{bmatrix} \end{aligned}$$

Matching like powers in the invariance equations gives that the homological equation has the desired form

$$[DF(p_0) - \lambda^n \mathrm{Id}_{2N\times 2N}]\, p_n = b_n, \tag{18}$$

for $n \geq 2$, where b_n is given by

$$b_n = \begin{pmatrix} b_n^{(N)} \\ b_n^{(1)} \\ \vdots \\ b_n^{(N-1)} \end{pmatrix}$$

and

$$b_n^{(k)} = \begin{pmatrix} \frac{-a}{n} \sum_{j=1}^{n-1} j c_{n-j}^{(k)} p_{n,2}^{(k)} \\ \frac{-a}{n} \sum_{j=1}^{n-1} j c_{n-j}^{(k)} p_{n,2}^{(k)} \end{pmatrix},$$

for $1 \leq k \leq N$.

Note that once $(p_{n,1}^{(k)}, p_{n,2}^{(k)})$ are computed as the components of the solution of the n-th homological Equation (18), then $s_{n+1}^{(k)}$, and $c_{n+1}^{(k)}$ are computed and stored for use in the solution of the $n+1$-th homological equation. The automatic differentiation scheme just described allow us to compute the power series coefficients of the composition $\sin(P_2^{(k)}(\theta))$ for the cost of two Cauchy products. However, this approach requires us to store the coefficients $s_n^{(k)}$ and $c_n^{(k)}$ throughout the computation.

3.2.5 Further remarks on automatic differentiation: nonlinearities given by the elementary functions of mathematical physics

The procedure discussed in Section 3.2.4 can be made quite general. We elaborate briefly below, but the interested reader should also consult [61, 60, 62, 63, 64] for more complete discussion. In particular, the first reference describes a general algorithmic framework for manipulation of power series manipulation in nonlinear problems. The idea is that many of the so called *elementary functions of mathematical physics*, which make up the nonlinear terms in many applied problems, are themselves solutions of simple differential equations. This lets one extend the ideas exploited in Section 3.2.4 to many other situations.

To formalize the discussion suppose

$$P(\theta) = \sum_{n=0}^{\infty} p_n \theta^n, \qquad Q(\theta) = \sum_{n=0}^{\infty} q_n \theta^n, \qquad R(\theta) = \sum_{n=0}^{\infty} r_n \theta^n,$$

are power series with $p_n, q_n, r_n \in \mathbb{C}$, for $n \geq 0$. The following gives a list several useful results for some common nonlinear functions.

- **Addition:** If $R(\theta) = P(\theta) + Q(\theta)$ then

$$r_n = p_n + q_n.$$

- **Multiplication:** If $R(\theta) = P(\theta)Q(\theta)$ then

$$r_n = \sum_{k=0}^{n} p_{n-k} q_k.$$

- **Division:** If $R(\theta) = P(\theta)/Q(\theta)$ then

$$r_n = \frac{1}{q_0} \left(p_n - \sum_{k=1}^{n} r_{n-k} q_k \right).$$

- **Powers:** If $\alpha \in \mathbb{C}$ and $R(\theta) = P(\theta)^\alpha$ then

$$r_n = \frac{1}{n p_0} \sum_{k=0}^{n-1} (n\alpha - k(\alpha + 1)) p_{n-k} r_k.$$

- **The natural exponential:** If $R(\theta) = e^{P(\theta)}$, then

$$r_n = \frac{1}{n}\sum_{k=0}^{n-1}(n-k)p_{n-k}r_k.$$

- **The natural logarithm:** If $R(\theta) = \log P(\theta)$, then

$$r_n = \frac{1}{p_0}\left(p_n - \frac{1}{n}\sum_{k=1}^{n-1}(n-k)r_{n-k}p_k.\right)$$

- **Sine and cosine:** If $R(\theta) = \sin(P(\theta))$ and $Q(\theta) = \cos(P(\theta))$ then

$$r_n = \frac{-1}{n}\sum_{k=1}^{n} kq_{n-k}p_k,$$

and

$$q_n = \frac{1}{n}\sum_{k=1}^{n} kr_{n-k}p_k.$$

See [61] for proofs. Using these formulas one could apply the techniques of the present work to any map with nonlinearities given by the elementary functions. Moreover, similar recursion can be obtained for other elementary functions such as Bessel functions, elliptic integrals, etcetera.

4 Numerical implementation and example computations

The results of the previous section lead to numerical procedures as follows: for a period N orbit, find the m stable (or unstable) eigenvalues, and compute associated eigenvectors. This last involves an arbitrary choice of the scalings. Suppose that polynomial approximation to order $K \geq 2$ is desired, and that the eigenvalues are non-resonant. Then solve the homological equations in increasing order 2, 3, ..., up to K. This leads a collection of polynomials $P_K^1, \ldots, P_K^N \colon \mathbb{R}^m \to \mathbb{R}^M$.

The K-th order polynomials $P_K^j \colon \mathbb{R}^m \to \mathbb{R}^M$ for $1 \leq j \leq m$ are defined and analytic on all of $\mathbb{R}^m$. Of course we cannot expect the associated truncation error small on all $\mathbb{R}^m$, and we always restrict to a *numerical domain* on which the approximation should be considered reasonable. Recall that by Claim 3 from Section 3.1, we are free to fix the numerical domain as $B_1^m(0) \subset \mathbb{R}^m$, and choose the scalings of the eigenvectors so that the polynomial is well behaved on this domain. Evaluating the polynomials only for variables smaller than one leads to numerically stable results.

The only remaining question is: how to choose the scalings of the eigenvectors? We would like to choose these scalings as large as possible so as to parameterize large regions of the stable/unstable manifold and hence learn as much as possible about the manifolds far from the periodic orbit. On the other hand, we also want the approximation to be reliable on $B_1^m(0)$. In order to quantify the notion of reliability we define the *a-posteriori error* associated with the the polynomials $P_K^1, \ldots, P_K^N$ to be the positive number

$$\varepsilon_K := \max_{1\leq j\leq M}\left(\sup_{\theta\in B_1^m(0)}\left\|f(P_K^j(\theta_1,\ldots,\theta_m)) - P_K^{j+1}(\lambda_1\theta_1,\ldots,\lambda_m\theta_m)\right\|\right), \tag{19}$$

where we let $P_K^{N+1}(\theta) = P_K^1(\theta)$, i.e. impose periodicity. If the a-posteriori error associated with P_K is small this means that the conjugacy is approximately satisfied and we are reasonable confident (but not certain) that our approximation is good.

The following describes an algorithm which, given an approximation order K and a desired numerical numerical tolerance ϵ_{tol}, adaptively rescales the eigenvectors until the scalings are as large as possible without exceeding the numerical tolerance. The discussion in the next section sheds further light on the procedure.

- **Inputs:** Choose a period N orbit, and compute its eigenvectors scaled initially to length one. Fix a tolerance ϵ_{tol} and a polynomial order of approximation K.
- **Step 1:** Compute the Taylor coefficients of P^1, ..., P^N by solving the homological equations to order K.
- **Step 2:** Evaluate the a-posteriori error ε_K defined in Equation (19). (Or as discussed in Remark 4.1 below).
- **Step 3:** If $\varepsilon_K < \epsilon_{\text{tol}}$ then the scale is increased and step 2 is repeated. If $\epsilon_{\text{tol}} \leq \varepsilon_K$ then the scale is decreased.

  Repeat until ε_K is below but within (for example) ninety five percent of ϵ_{tol}.

Remark 4.1 (Analytic norms)**.** In practice we can obtain efficient numerical bounds on the a-posteriori error by computing only on the level of the coefficients. In fact if $g\colon \mathbb{C}^m \to \mathbb{C}$ is analytic on the unit poly-disk

$$D_1^m(0) := \left\{ z = (z_1, \ldots, z_m) \in \mathbb{C}^m \mid \max_{1 \leq j \leq m} |z_j| < 1 \right\},$$

then by the maximum modulus principle and the triangle inequality we have

$$\sup_{\theta \in B_1^m(0)} |g(\theta)| \leq \sup_{z \in \partial D_1^m(0)} |g(z)| \leq \sum_{n=0}^{\infty} |g_n|,$$

where $g_n \in \mathbb{C}$ are the powerseries coefficients of g. Note that the inequality above holds even when one or more of the quantities are infinite. The final quantity on the right is an ℓ^1 norm on the Taylor coefficient, sometimes referred to as an analytic norm.

Consider the a-posteriori error in Equation (19) in the case that f is a polynomial. Then $f(P_K^j(\theta_1, \ldots, \theta_m)$ and $P^{j+1}(\lambda_1\theta_1, \ldots, \lambda_m\theta_m)$ are both polynomials so that

$$f(P_K^j(\theta_1, \ldots, \theta_m)) - P_K^{j+1}(\lambda_1\theta_1, \ldots, \lambda_m\theta_m) = \sum_{|\alpha|=0}^{\hat{K}} e_\alpha \theta^\alpha,$$

for some $e_\alpha \in \mathbb{R}^M$. More over the coefficients e_α are computed at the cost of an evaluation of f (on a polynomial). Then we can bound the a-posteriori error by

$$\varepsilon_K \leq \sum_{|\alpha|=0}^{\hat{K}} \|e_\alpha\|.$$

If $P_K^1, \ldots, P_K^N$ are good approximations then the coefficients e_α will be small and this provides a good bound. If f is not a polynomial then we must include a Taylor remainder bound in the estimates above.

4.1 Non-uniqueness and choosing the lengths of the eigenvectors: decay rates of the Taylor coefficients

In order to illustrate the numerical considerations in a concrete example we consider the simple case of parametrizing the stable and unstable manifolds attached to a saddle type period 2 point for the Hénon Map. Recall the Hénon map given in Equation (11). If $p_1, p_2 \in \mathbb{R}^2$ is a period two orbit then, as soon as we choose eigenvectors, the parameterizations of the local stable/unstable manifolds are determined by solving the homological Equation (13) to any desired order.

Suppose for example we compute the polynomial approximation to order $K = 100$, and that we make the seemingly natural choice of scaling the eigenvector to have Euclidean norm one. The resulting polynomial approximations are plotted in the top frame of Figure 4, over the domain $B_1^1(0) = [-1, 1]$. The local manifolds have order one size in phase space. But consider the decay rates of the stable/unstable manifold coefficients: the magnitudes of the Taylor coefficients are plotted log base ten in the bottom frame of Figure 4. We see that the magnitudes decrease exponentially fast to order ten to the negative several hundred in both the stable (left/red) and unstable (right/blue) cases.

Better results are obtained by choosing a larger scaling for the eigenvectors. With $K = 100$, and the Taylor coefficient found in the last example we proceed as follows. We fix prescribed numerical tolerances (somewhat arbitrarily) of $\epsilon_{\text{tol}} = (10^-14$ for the stable manifold and 10^{-10} for the unstable manifold). Now we apply the scaling search algorithm and obtain, after five steps, an eigenvector scaling of $s = 4.94$ for the unstable manifold and $s = 5$ for the stable manifold. Plots of the resulting local stable/unstable manifolds are illustrated in the top frame of Figure 5. Here we see much larger portions of the manifolds. Indeed these local manifolds already intersect several times and are beginning to give the classical shape of the attractor. The decay of the magnitude of the Taylor coefficients are plotted log base ten in the bottom frames of Figure 5 (stable is left/red and unstable right/blue).

Note that in the last example a substantial portion of the coefficients have magnitude smaller than machine epsilon, and we might guess that we have over computed, i.e. that we can obtain the same results with a smaller number of coefficients. For example, by around $K = 30$, the magnitude of the of the Taylor coefficients is on the order of 10^{-16}.

So, we repeat the computation approximating with polynomials of order $N = 30$. Using the adaptive scheme to choose the largest scaling possible now gives an a-posteriori error less than $\epsilon_{\text{tol}} = 10^{-14}$ for the stable manifold and $\epsilon_{\text{tol}} = 10^{-10}$ for the unstable manifold. However, the optimal scaling is only $s = 2.178$. The resulting manifolds are shown in the top frame of Figure 6, with the scalings in log base ten in the bottom frames of the same figure.

Note that this computation is a little better than the computation with $K = 100$ and unit scaling, in that we see at least one point of homoclinic intersection, and at least one fold of the parameterized manifolds. But the results are much worse than those obtained using the $K = 100$ and the adaptive rescaling procedure. This suggests that the high Taylor modes in the computation just mentioned are playing a significant role in the a-posteriori error, even though they are much smaller than machine epsilon.

It is less clear how much of a role these high modes play in the precision of the plotted manifolds, i.e. in the phase space representation. This discussion illustrates the need for finer methods of a-posteriori analysis such as those mentioned already in Remark 1.2. We postpone such analysis to an upcoming work.

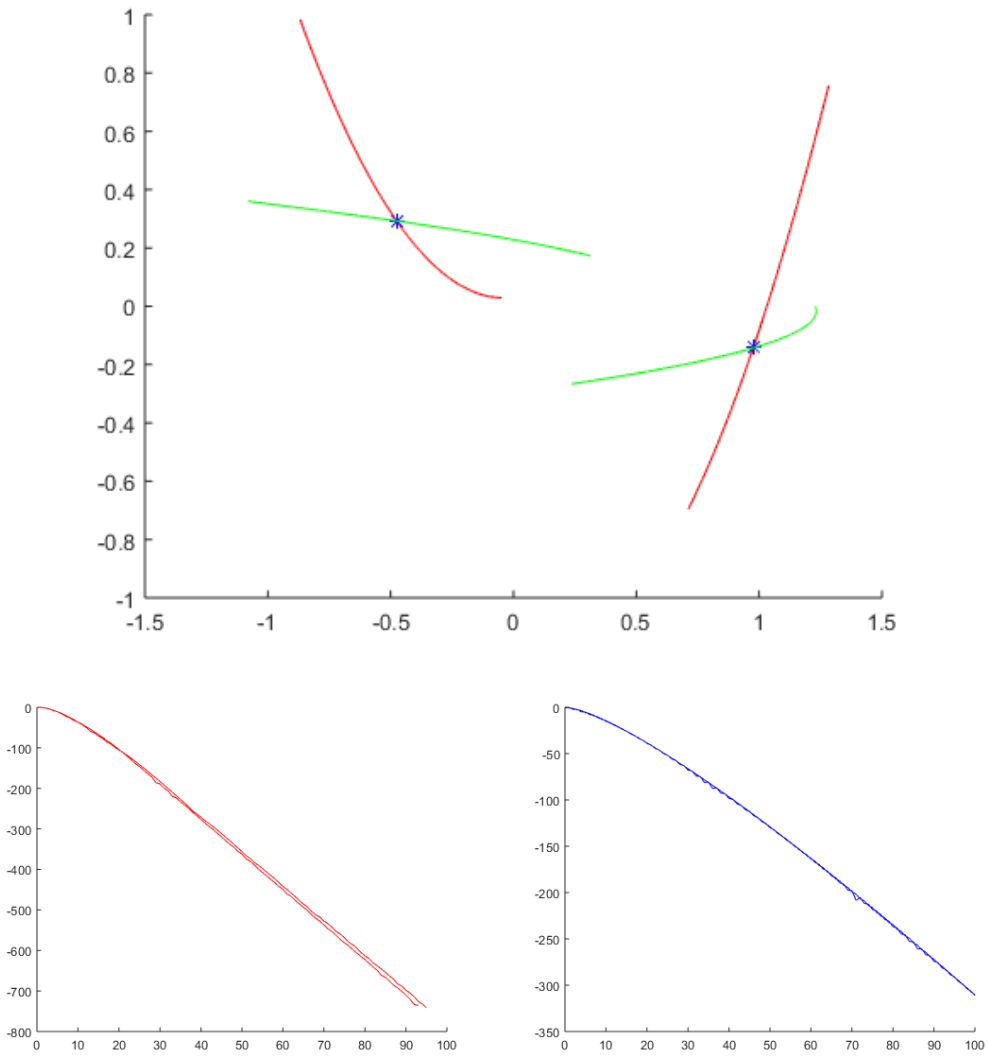

Figure 4: Manifolds attached to a period two for Hénon: classic parameter values, approximation order $N = 100$, and eigenvectors scaled to one. TOP: parameterized invariant manifolds, red stable and green unstable. BOTTOM LEFT: magnitude of Taylor coefficients of the unstable parameterization. BOTTOM RIGHT: magnitude of the coefficients of the stable parameterization. Both bottom plots have the $0 \leq n \leq N$ on the x-axis and $\log_{10}(\|p_n\|)$ on the y-axis.

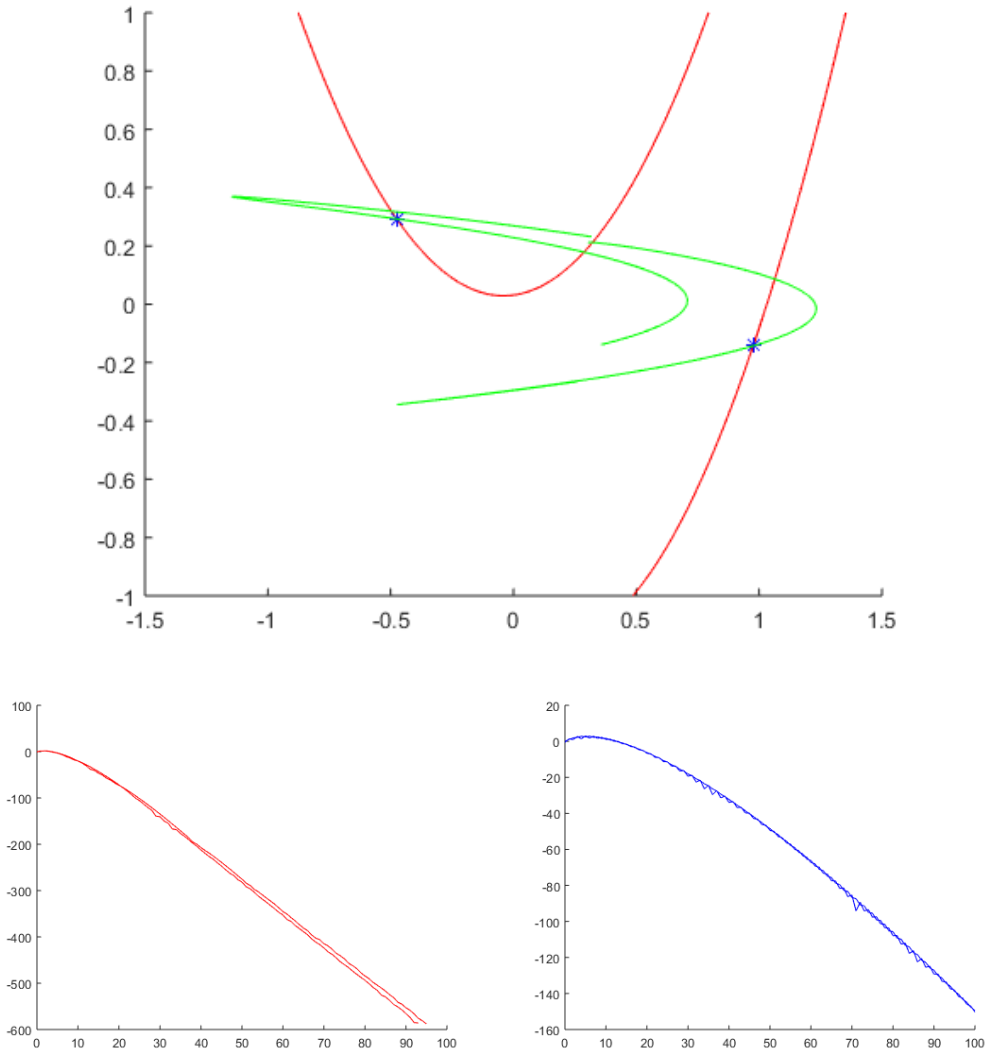

Figure 5: Manifolds attached to a period two for Hénon: classic parameter values, approximation order $K = 100$, and eigenvectors with optimal scaling. A-posteriori error held below 10^{-14} for the stable and 10^{-10} for the unstable manifolds TOP: parameterized invariant manifolds, red stable and green unstable. BOTTOM LEFT: magnitude of Taylor coefficients of the unstable parameterization. BOTTOM RIGHT: magnitude of the coefficients of the stable parameterization. Both bottom plots have the $0 \leq n \leq K$ on the x-axis and $\log_{10}(\|p_n\|)$ on the y-axis.

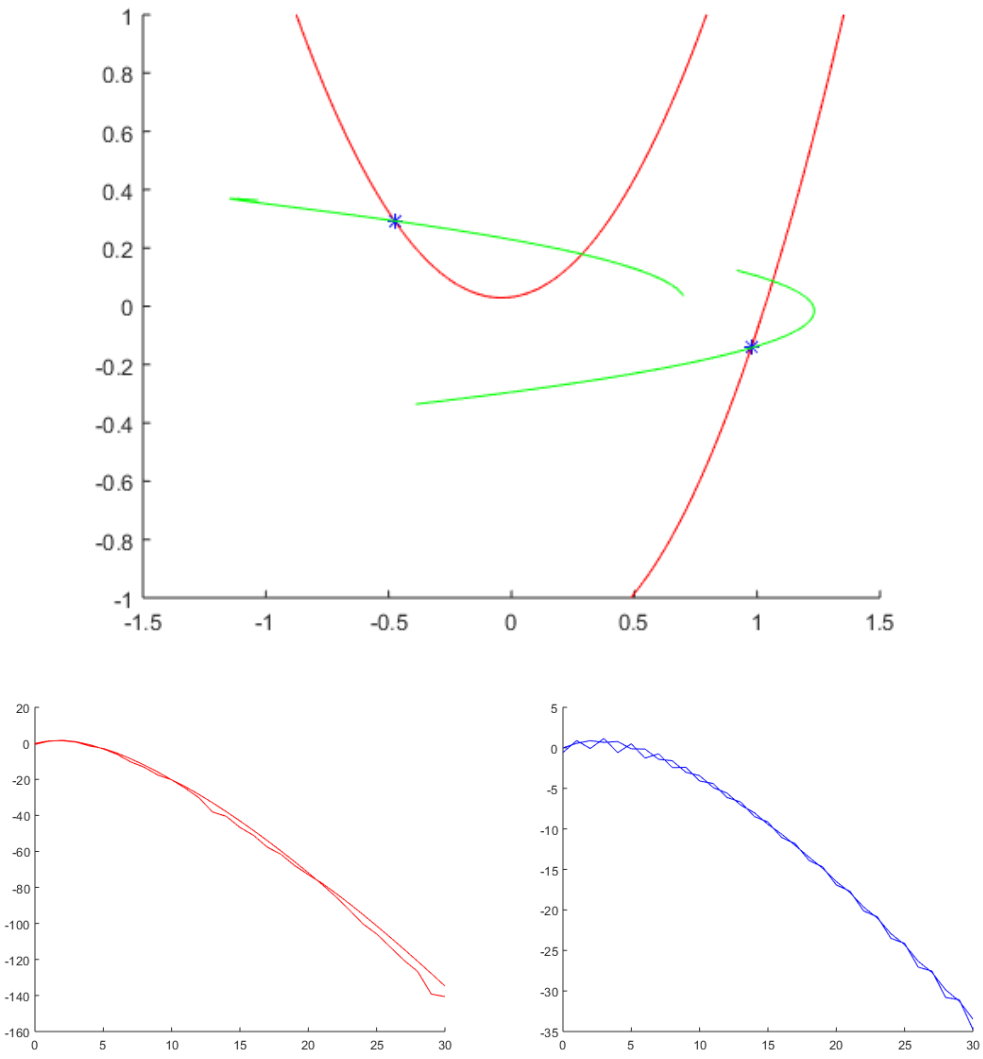

Figure 6: Manifolds attached to a period two for Hénon: classic parameter values, approximation order $K = 30$, and eigenvectors with optimal scaling. A-posteriori errors are the same as for $K = 100$ above. TOP: parameterized invariant manifolds, red stable and green unstable. BOTTOM LEFT: magnitude of Taylor coefficients of the unstable parameterization. BOTTOM RIGHT: magnitude of the coefficients of the stable parameterization. Both bottom plots have the $0 \leq n \leq K$ on the x-axis and $\log_{10}(\|p_n\|)$ on the y-axis.

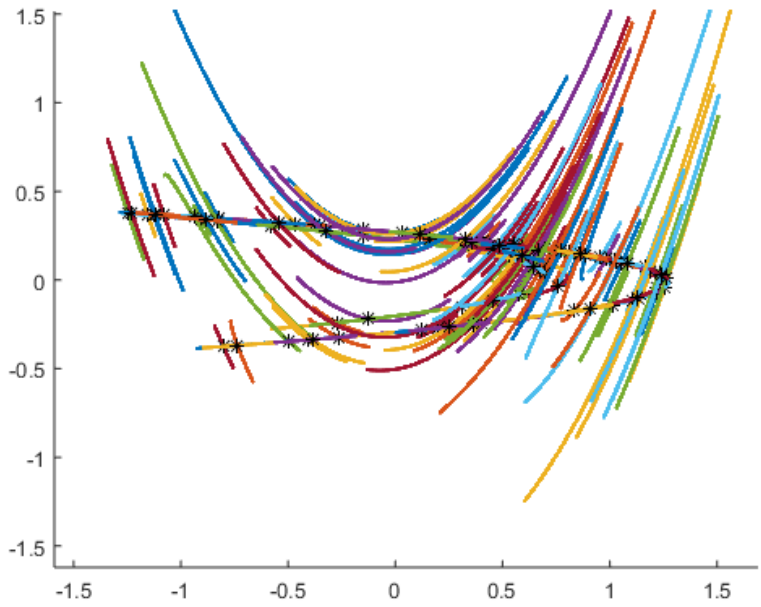

Figure 7: Manifolds attached to a period 95 orbit for Hénon: classic " parameter values, approximation order $N = 50$, and eigenvectors with optimal scaling. A-posteriori error held below 10^{-14}. Unstable manifolds are tangent to the attractor and stable manifolds are normal. Colors are chosen at random.

4.2 Long periodic orbits for the Hénon map

One strength or our algorithm is that it applies to much higher periods than two. Figure 7 illustrates the results of our procedure applied to a single orbit of period $M = 95$ for the Henon map with the classic parameters $a = 1.4$ and $b = 0.3$. The 2×95 parameterization functions are approximated to polynomial order $M = 50$, and we employ the adaptive rescaling algorithm with a desired tolerance of $\epsilon_{\text{tol}} = 10^{-14}$. The algorithm results in an eigenvector scaling of $s = 5.37$ for the stable and $s = 2.74$ for the unstable manifold.

Remark 4.2 (Finding orbits of long period)**.** In order to find periodic orbits (long or otherwise) for the Hénon map we proceed as follows. We pick any point "near" the attractor (say $x = 0$, $y = 1$) and iterate a large number of times (say $K = 10^5$ or more). Ignoring the first, say one hundred points on the resulting orbit segment, we have a collection of points near the attractor. We now search this collection for orbits which are approximately period M for every $2 \leq M \leq M_{\max}$. For the Hénon map we typically take $M_{\max} < 100$.

When we find an orbit segment which is approximately period M we run a Newton method to obtain a better orbit. We also check that the orbit we obtain has not already been found. If the orbit is new we add it to our list. This is a typical search procedure based on the notion that the dynamics on the attractor are uniquely ergodic, hence single long orbit should convey the same information as sampling "uniformly" over the attractor. The procedure just described was also used to find the orbits discussed in Remark 1.1 and illustrated in Figure 1.

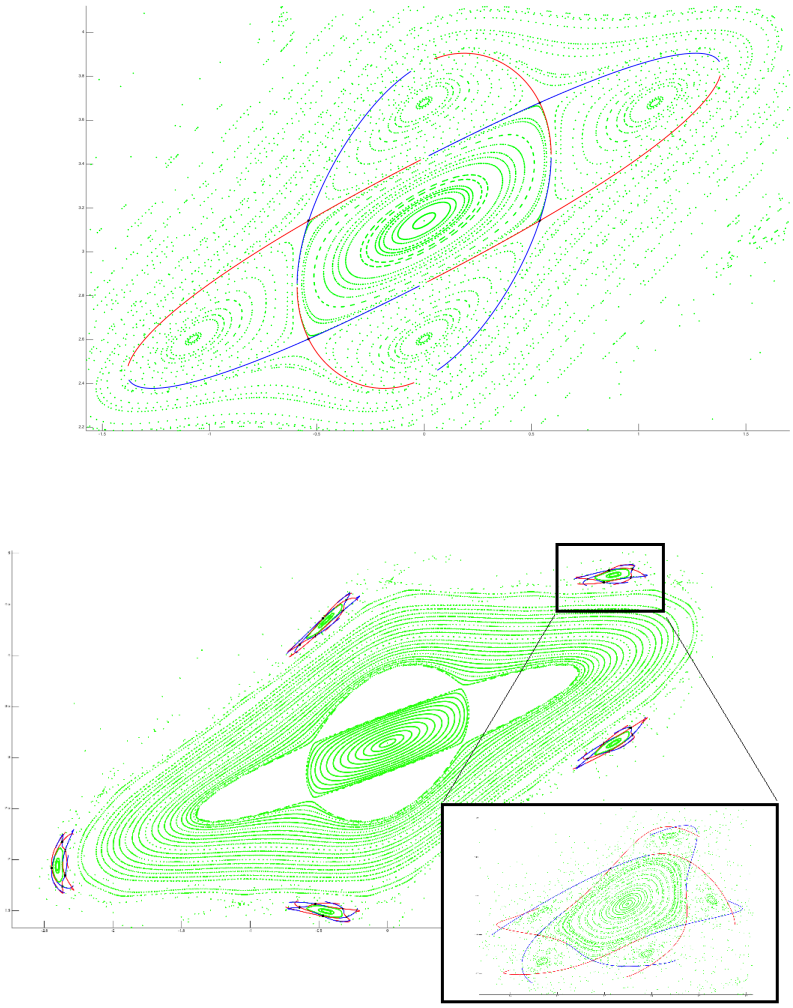

Figure 8: The standard map with $a = 2.1$: TOP: local stable and unstable manifolds attached to a period four orbit. BOTTOM: local stable and unstable manifolds attached to a period twenty five orbit. Inlay zooms in around a secondary torus and illustrates homoclinic intersection points. Unstable manifolds are blue and stable manifolds are red.

4.3 Long periodic orbits in the standard map

In this section we consider several example results for the Standard map given by Equation (17) with $a = 2.1$, i.e. far from the integrable/perturbative case. Recall that this map has transcendental nonlinearity given by the sine function. Once we choose a periodic orbit of period M we compute the Taylor coefficients by solving the homological equations given by Equation (18). For example, the top frame of Figure 8 illustrates the local unstable manifolds attached to a period 4 point approximated to polynomial order $N = 200$. The

eigenvector is scaled to $s = 1.6$.

The bottom frame of Figure 8 illustrates the stable/unstable manifolds attache to a period 25 orbit of the Standard map, again approximated to polynomial order $N = 200$. The stable and unstable manifolds are scaled by $s = 0.95$ and $s = 0.98$ respectively. The inlay in the figure "zooms in" on one of the KAM islands (or secondary tori) surrounding the primary family of invariant circles in the standard map. This island shows yet another layer of islands (or tertiary tori) and our period 25 orbit is the hyperbolic "twin" of the (presumed) period 25 elliptic orbit in the center of the tertiary tori. The local stable/unstable manifolds parameterized here already show homoclinic intersections.

Remark 4.3 (Finding long periodic orbits for the standard map)**.** The standard map is an area preserving map, hence it has no non-trivial attractor. The full map is not uniquely ergodic, and the strategy described in Remark 4.2 will not work. Moreover, simply sampling the phase space can be misleading, as there are many invariant circles which will be hard to distinguish from long periodic orbits numerically.

The orbits in the examples above are where found by "eyeballing" the phase space portrait and looking for interesting features. For example, looking only at the green points in Figure 8, the dominant feature is the period four KAM islands around the primary family of circles about the origin.

Standard results for area preserving maps tell us to expect an elliptic period four orbit in the middle of these islands, and that the elliptic period four point should have an associated hyperbolic period four orbit. Simply inspecting the picture suggests that one point near this orbit is $x = -0.5$, $y = 2.5$. Simply running a Newton method with this as the initial condition converges to a period 4 point to machine precision. Then computing the eigenvectors and solving the homological equations is straight forward. The initial guess for the period 25 orbit was obtained in precisely the same manner.

4.4 Period four vortex bubble in the Lomelí map

In the planar examples mentioned in the previous sections, one can learn a great deal about the dynamics of the system simply by phase space sampling. For example iterating almost any initial point in the plane for long enough under the Hénon map yields the familiar picture of of the attractor. Similarly, the green points in Figures 8 give a reasonable impression of the dynamics is the standard map for $a = 2.1$.

For dissipative maps of $\mathbb{R}^3$ things are not so different. Such maps have attractors and simply iterating points often provides a good picture of the dynamics. For volume preserving maps of $\mathbb{R}^3$ the situation is somewhat less clear.

Consider for example the Lomelí map given by Equation (14). Plotting a typical bounded orbit of the system leads to an amorphous blob. And plotting many such orbits leads to a true point cloud which tells us very little. The system however does admit many invariant tori.

Figure 9 for example illustrates a number of orbits for the system with parameters $a = 0.5$, $b = -0.5$, $c = 1$, $\tau = 1.333333333$, and $\alpha = 0.3444444444$. These orbits illustrate some period four invariant tori, secondary period four tori (or invariant circles?) about these, and finally a single invariant torus enclosing the entire structure. For each object we are simply iterating a single point which is presumably near the invariant torus or circle. So there is no parameterization of these manifolds.

Moreover, these orbits are not "typical": rather they were identified by eye as "interesting" results from a rather larger sampling of phase space. Such a search is both time consuming and ad-hoc. Nevertheless it yields some interesting period four structure. The reader

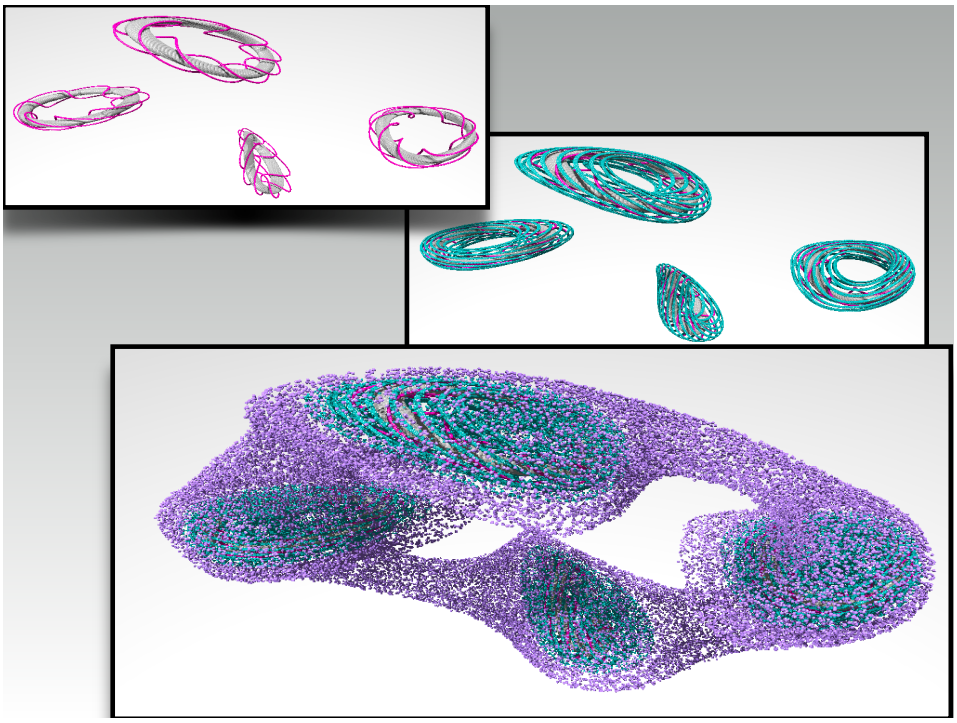

Figure 9: Quasi-periodic invariant objects for the Lomelí Map: TOP LEFT: period four invariant tori encircled by invariant circles. MIDDLE RIGHT: same tori with longer invariant circles. BOTTOM: period one invariant torus encasing the period four structure. All of these invariant structures were located by phase space sampling.

interested in the dynamics of the Lomelí map may want to review the works of [54, 55, 11, 56, 12, 65]. Indeed the period four tori discussed here are also seen in the forth reference just cited.

This strategy, simply iterating points and examining the results for structure, will not directly tell us anything about hyperbolic objects. However, based on these results we can *guess* that there should be a pair of hyperbolic period four points near the top and bottom of the opening of the period four torus. Similarly we can guess (or work out directly by hand) that there are a pair of fixed points near the top and bottom of the opening of the larger surrounding torus.

Once we have located the period four points (or fixed points) then it is a simple procedure to compute the corresponding eigenvectors and solve the homological equations for the one and two dimensional stable/unstable manifolds attached to them. These parameterized local manifolds, when combined with the quasi-periodic structures found through phase space sampling, provide substantial insight into the phase space structure of the system.

References

[1] X. Cabré, E. Fontich, and R. de la Llave. The parameterization method for invariant manifolds. I. Manifolds associated to non-resonant subspaces. *Indiana Univ. Math. J.*, 52(2):283–328, 2003.

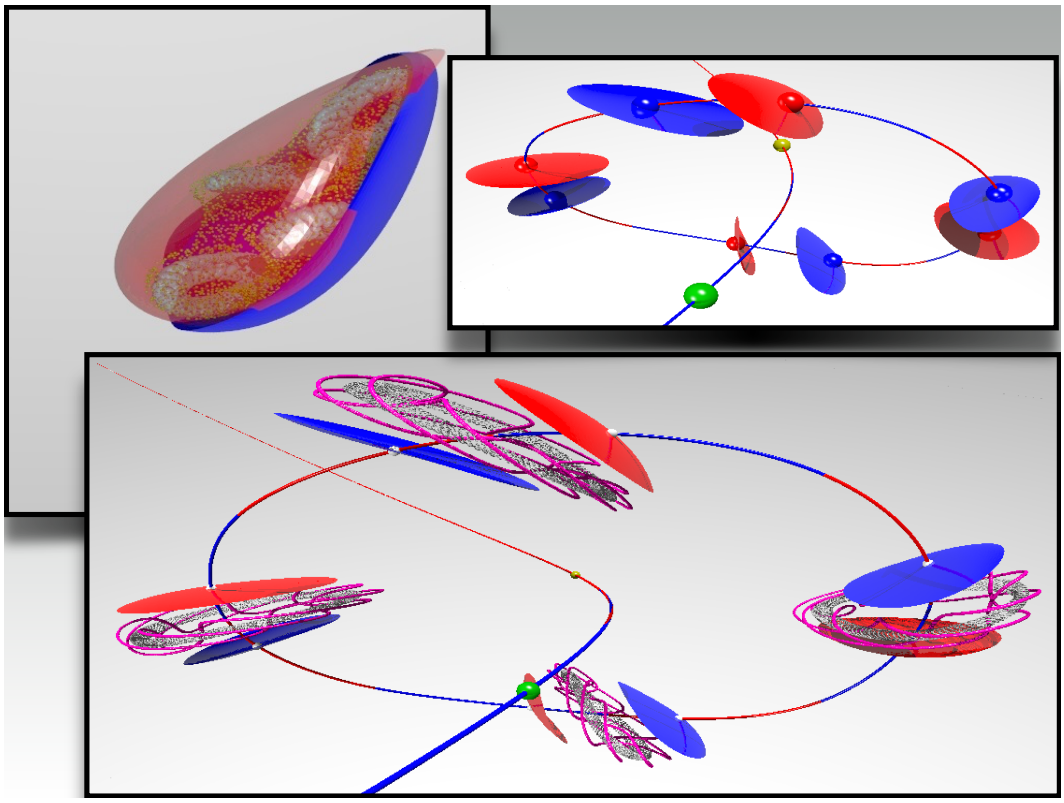

Figure 10: Hyperbolic invariant objects for the Lomelí map: TOP LEFT: 2d local stable/unstable manifolds of the fixed points. Quasi periodic invariant tori (period one and four) seen inside. TOP RIGHT: 1d stable/unstable manifolds attached to the fixed points (green and yellow spheres). Also 1d and 2d stable/unstable manifolds attached to the period four points. BOTTOM: the stable/unstable manifolds of fixed points and period four orbit along with the period four invariant tori.

[2] X. Cabré, E. Fontich, and R. de la Llave. The parameterization method for invariant manifolds. II. Regularity with respect to parameters. *Indiana Univ. Math. J.*, 52(2):329–360, 2003.

[3] X. Cabré, E. Fontich, and R. de la Llave. The parameterization method for invariant manifolds. III. Overview and applications. *J. Differential Equations*, 218(2):444–515, 2005.

[4] Tomas Johnson and Warwick Tucker. A note on the convergence of parametrised non-resonant invariant manifolds. *Qual. Theory Dyn. Syst.*, 10(1):107–121, 2011.

[5] J. D. Mireles James and Konstantin Mischaikow. Rigorous a posteriori computation of (un)stable manifolds and connecting orbits for analytic maps. *SIAM J. Appl. Dyn. Syst.*, 12(2):957–1006, 2013.

[6] J. D. Mireles James. Computer assisted error bounds for linear approximation of (un)stable manifolds and rigorous validation of higher dimensional transverse connect-

ing orbits. *Communications in Nonlinear Science and Numerical Simulation*, 22(1-3):1102–1133, 2015.

[7] M. Breden, J.P. Lessard, and J.D. Mireles James. Computation of maximal local (un)stable manifold patches by the parameterization method. *Indagationes Mathematicae*, 27(1):340–367, 2016.

[8] J. B. Van den Berg, J. D. Mireles James, and Christian Reinhardt. Computing (un)stable manifolds with validated error bounds: non-resonant and resonant spectra. *Journal of Nonlinear Science*, 26:1055–1095, 2016.

[9] J. D. Mireles James. Fourier-taylor approximation of unstable manifolds for compact maps: numerical implementation and computer assisted error bounds. *(to appear in Foundations of Computational Mathematics)*, 2016.

[10] Clark Robinson. *Dynamical systems*. Studies in Advanced Mathematics. CRC Press, Boca Raton, FL, 1995. Stability, symbolic dynamics, and chaos.

[11] J. D. Mireles James and Hector Lomelí. Computation of heteroclinic arcs with application to the volume preserving Hénon family. *SIAM J. Appl. Dyn. Syst.*, 9(3):919–953, 2010.

[12] J. D. Mireles James. Quadratic volume-preserving maps: (un)stable manifolds, hyperbolic dynamics, and vortex-bubble bifurcations. *J. Nonlinear Sci.*, 23(4):585–615, 2013.

[13] J.D. Mireles James. Polynomial approximation of one parameter families of (un)stable manifolds with rigorous computer assisted error bounds. *Indagationes Mathematicae*, 26(1):225–265, 2015.

[14] S. Anastassiu, T. Bountis, and Arnd Bäcker. Homoclinic points of 2-d and 4-d maps via the parameterization method. *(Submitted)* `https://arxiv.org/abs/1605.05521`, 2016.

[15] A. Haro, M. Canadell, J-LL. Figueras, A. Luque, and J-M. Mondelo. *The parameterization method for invariant manifolds: from rigorous results to effective computations*, volume -. Springer, 2016. Preprint `http://www.maia.ub.es/~alex`.

[16] Rafael de la Llave and J.D. Mireles James. Parameterization of invariant manifolds by reducibility for volume preserving and symplectic maps. *Discrete Contin. Dyn. Syst.*, 32(12):4321–4360, 2012.

[17] Valter Franceschini and Lucio Russo. Stable and unstable manifolds of the Hénon mapping. *J. Statist. Phys.*, 25(4):757–769, 1981.

[18] C. Simo. On the Analytical and Numerical Approximation of Invariant Manifolds. In D. Benest and C. Froeschle, editors, *Modern Methods in Celestial Mechanics, Comptes Rendus de la 13ieme Ecole Printemps d'Astrophysique de Goutelas (France), 24-29 Avril, 1989. Edited by Daniel Benest and Claude Froeschle. Gif-sur-Yvette: Editions Frontieres, 1990., p.285*, page 285, 1990.

[19] Wolf-Jürgen Beyn and Winfried Kleß. Numerical Taylor expansions of invariant manifolds in large dynamical systems. *Numer. Math.*, 80(1):1–38, 1998.

[20] Bernd Krauskopf and Hinke Osinga. Globalizing two-dimensional unstable manifolds of maps. *Internat. J. Bifur. Chaos Appl. Sci. Engrg.*, 8(3):483–503, 1998.

[21] Bernd Krauskopf and Hinke Osinga. Growing 1D and quasi-2D unstable manifolds of maps. *J. Comput. Phys.*, 146(1):404–419, 1998.

[22] Bernd Krauskopf and Hinke M. Osinga. Computing geodesic level sets on global (un)stable manifolds of vector fields. *SIAM J. Appl. Dyn. Syst.*, 2(4):546–569 (electronic), 2003.

[23] Bernd Krauskopf and Hinke M. Osinga. The Lorenz manifold as a collection of geodesic level sets. *Nonlinearity*, 17(1):C1–C6, 2004. With multimedia enhancements available from the abstract page in the online journal.

[24] John Guckenheimer and Alexander Vladimirsky. A fast method for approximating invariant manifolds. *SIAM J. Appl. Dyn. Syst.*, 3(3):232–260, 2004.

[25] B. Krauskopf, H. M. Osinga, E. J. Doedel, M. E. Henderson, J. Guckenheimer, A. Vladimirsky, M. Dellnitz, and O. Junge. A survey of methods for computing (un)stable manifolds of vector fields. *Internat. J. Bifur. Chaos Appl. Sci. Engrg.*, 15(3):763–791, 2005.

[26] Michael E. Henderson. Computing invariant manifolds by integrating fat trajectories. *SIAM J. Appl. Dyn. Syst.*, 4(4):832–882 (electronic), 2005.

[27] Michael Dellnitz and Andreas Hohmann. A subdivision algorithm for the computation of unstable manifolds and global attractors. *Numer. Math.*, 75(3):293–317, 1997.

[28] Roy H. Goodman and Jacek K. Wróbel. High-order bisection method for computing invariant manifolds of two-dimensional maps. *Internat. J. Bifur. Chaos Appl. Sci. Engrg.*, 21(7):2017–2042, 2011.

[29] Jacek K. Wróbel and Roy H. Goodman. High-order adaptive method for computing two-dimensional invariant manifolds of three-dimensional maps. *Commun. Nonlinear Sci. Numer. Simul.*, 18(7):1734–1745, 2013.

[30] Pablo Aguirre, Eusebius J. Doedel, Bernd Krauskopf, and Hinke M. Osinga. Investigating the consequences of global bifurcations for two-dimensional invariant manifolds of vector fields. *Discrete Contin. Dyn. Syst.*, 29(4):1309–1344, 2011.

[31] Eusebius J. Doedel, Bernd Krauskopf, and Hinke M. Osinga. Global invariant manifolds in the transition to preturbulence in the Lorenz system. *Indag. Math. (N.S.)*, 22(3-4):222–240, 2011.

[32] Jennifer L. Creaser, Bernd Krauskopf, and Hinke M. Osinga. α-flips and T-points in the Lorenz system. *Nonlinearity*, 28(3):R39–R65, 2015.

[33] Pablo Aguirre, Bernd Krauskopf, and Hinke M. Osinga. Global invariant manifolds near a Shilnikov homoclinic bifurcation. *J. Comput. Dyn.*, 1(1):1–38, 2014.

[34] Stefanie Hittmeyer, Bernd Krauskopf, and Hinke M. Osinga. Interactions of the Julia set with critical and (un)stable sets in an angle-doubling map on $\mathbb{C}\backslash\{0\}$. *Internat. J. Bifur. Chaos Appl. Sci. Engrg.*, 25(4):1530013, 36, 2015.

[35] Michael Dellnitz, Oliver Junge, Wang Sang Koon, Francois Lekien, Martin W. Lo, Jerrold E. Marsden, Kathrin Padberg, Robert Preis, Shane D. Ross, and Bianca Thiere. Transport in dynamical astronomy and multibody problems. *Internat. J. Bifur. Chaos Appl. Sci. Engrg.*, 15(3):699–727, 2005.

[36] W. S. Koon, M. W. Lo, J. E. Marsden, and S. D. Ross. Low energy transfer to the moon. *Celestial Mech. Dynam. Astronom.*, 81(1-2):63–73, 2001. Dynamics of natural and artificial celestial bodies (Poznań, 2000).

[37] G. Gómez, W. S. Koon, M. W. Lo, J. E. Marsden, J. Masdemont, and S. D. Ross. Connecting orbits and invariant manifolds in the spatial restricted three-body problem. *Nonlinearity*, 17(5):1571–1606, 2004.

[38] Marco Tantardini, Elena Fantino, Yuan Ren, Pierpaolo Pergola, Gerard Gómez, and Josep J. Masdemont. Spacecraft trajectories to the L_3 point of the Sun-Earth three-body problem. *Celestial Mech. Dynam. Astronom.*, 108(3):215–232, 2010.

[39] J. J. Masdemont. High-order expansions of invariant manifolds of libration point orbits with applications to mission design. *Dyn. Syst.*, 20(1):59–113, 2005.

[40] Edward Belbruno, Marian Gidea, and Francesco Topputo. Weak stability boundary and invariant manifolds. *SIAM J. Appl. Dyn. Syst.*, 9(3):1061–1089, 2010.

[41] Amadeu Delshams, Marian Gidea, and Pablo Roldán. Transition map and shadowing lemma for normally hyperbolic invariant manifolds. *Discrete Contin. Dyn. Syst.*, 33(3):1089–1112, 2013.

[42] E. Belbruno, M. Gidea, and F. Topputo. Geometry of weak stability boundaries. *Qual. Theory Dyn. Syst.*, 12(1):53–66, 2013.

[43] Amadeu Delshams, Marian Gidea, Rafael de la Llave, and Tere M. Seara. Geometric approaches to the problem of instability in Hamiltonian systems. An informal presentation. In *Hamiltonian dynamical systems and applications*, NATO Sci. Peace Secur. Ser. B Phys. Biophys., pages 285–336. Springer, Dordrecht, 2008.

[44] M. Romero-Gómez, E. Athanassoula, J. J. Masdemont, and C. García-Gómez. Invariant manifolds as building blocks for the formation of spiral arms and rings in barred galaxies. In *Chaos in astronomy*, Astrophys. Space Sci. Proc., pages 85–92. Springer, Berlin, 2009.

[45] Mercè Romero-Gómez, Patricia Sánchez-Martín, and Josep J. Masdemont. How invariant manifolds form spirals and rings in barred galaxies. *Butl. Soc. Catalana Mat.*, 29(1):51–75, 110, 2014.

[46] H. E. Lomelí and J. D. Meiss. Resonance zones and lobe volumes for exact volume-preserving maps. *Nonlinearity*, 22(8):1761–1789, 2009.

[47] H. E. Lomelí and J. D. Meiss. Heteroclinic intersections between invariant circles of volume-preserving maps. *Nonlinearity*, 16(5):1573–1595, 2003.

[48] Héctor E. Lomelí, James D. Meiss, and Rafael Ramírez-Ros. Canonical Melnikov theory for diffeomorphisms. *Nonlinearity*, 21(3):485–508, 2008.

[49] Eusebius J. Doedel and Mark J. Friedman. Numerical computation of heteroclinic orbits. *J. Comput. Appl. Math.*, 26(1-2):155–170, 1989. Continuation techniques and bifurcation problems.

[50] Mark J. Friedman and Eusebius J. Doedel. Numerical computation and continuation of invariant manifolds connecting fixed points. *SIAM J. Numer. Anal.*, 28(3):789–808, 1991.

[51] W.-J. Beyn. The numerical computation of connecting orbits in dynamical systems. *IMA J. Numer. Anal.*, 10(3):379–405, 1990.

[52] E. J. Doedel. Lecture notes on numerical analysis of bifurcation problems. In *International Course on Bifurcations and Stability in Structural Engineering*. Université Pierre et Marie Curie (Paris VI), November 2000.

[53] M. Hénon. A two-dimensional mapping with a strange attractor. *Comm. Math. Phys.*, 50(1):69–77, 1976.

[54] Héctor E. Lomelí and James D. Meiss. Quadratic volume-preserving maps. *Nonlinearity*, 11(3):557–574, 1998.

[55] K. E. Lenz, H. E. Lomelí, and J. D. Meiss. Quadratic volume preserving maps: an extension of a result of Moser. *Regul. Chaotic Dyn.*, 3(3):122–131, 1998. J. Moser at 70 (Russian).

[56] H. R. Dullin and J. D. Meiss. Quadratic volume-preserving maps: invariant circles and bifurcations. *SIAM J. Appl. Dyn. Syst.*, 8(1):76–128, 2009.

[57] Boris V. Chirikov. A universal instability of many-dimensional oscillator systems. *Phys. Rep.*, 52(5):264–379, 1979.

[58] J. M. Greene, R. S. MacKay, F. Vivaldi, and M. J. Feigenbaum. Universal behaviour in families of area-preserving maps. *Phys. D*, 3(3):468–486, 1981.

[59] R. S. MacKay. A renormalisation approach to invariant circles in area-preserving maps. *Phys. D*, 7(1-3):283–300, 1983. Order in chaos (Los Alamos, N.M., 1982).

[60] Donald E. Knuth. *The art of computer programming. Vol. 2*. Addison-Wesley Publishing Co., Reading, Mass., second edition, 1981. Seminumerical algorithms, Addison-Wesley Series in Computer Science and Information Processing.

[61] Àngel Jorba and Maorong Zou. A software package for the numerical integration of ODEs by means of high-order Taylor methods. *Experiment. Math.*, 14(1):99–117, 2005.

[62] A. Haro. Automatic differentiation methods in computational dynamical systems: Invariant manifolds and normal forms of vector fields at fixed points. *Manuscript*.

[63] Martin Bücker, George Corliss, Paul Hovland, Uwe Naumann, and Boyana Norris, editors. *Automatic differentiation: applications, theory, and implementations*, volume 50 of *Lecture Notes in Computational Science and Engineering*. Springer-Verlag, Berlin, 2006. Papers from the 4th International Conference on Automatic Differentiation held in Chicago, IL, July 20–24, 2004.

[64] Warwick Tucker. *Validated numerics*. Princeton University Press, Princeton, NJ, 2011. A short introduction to rigorous computations.

[65] Maciej Capiński and J. D. Mireles James. Validated computation of heteroclinic sets. *(Submitted)*, 2016.